university of groningen

faculty of mathematics and natural sciences

The AdS/CFT correspondence and the quark-gluon plasma

Determining the viscosity to entropy density ratio of a strongly coupled fluid

Abstract

This thesis looks at the AdS/CFT correspondence as a method to determine dynamical properties of a strongly coupled plasma. These properties can in general not be determined by conventional methods like perturbation theory. We show how the correspondence can be used to determine the viscosity to entropy density ratio of a strongly coupled plasma. This gives the well known result: $\eta/s = 1/(4\pi)$. The correspondence might be useful to determine properties of the strongly coupled quark-gluon plasma. We know that the quark-gluon plasma is strongly coupled, despite previous believes that it is weakly coupled due to asymptotic freedom, because its viscosity to entropy density is small. The determined ratio from experiments is: $1/(4\pi) < \eta/s < 2.5/(4\pi)$, which means it is the most perfect fluid observed in nature. It is also remarkably close to the result of the AdS/CFT correspondence.

Bachelor Thesis in Physics

Author:
S. van der Woude

First supervisor:
dr. K. Papadodimas

Second supervisor:
prof. dr. D. Roest

July 8, 2015

Contents

1 Introduction

The theory of the strong interaction, quantum chromodynamics, has an interesting feature called asymptotic freedom. This means that the coupling constant becomes weaker for increasing energy. Asymptotic freedom makes the creation of a deconfined state, called the quark-gluon plasma, possible. The quark-gluon plasma is created in heavy-ion collisions. From these experiments we know that this state of matter is relatively strongly coupled, despite the asymptotic freedom. This strong coupling makes it extremely difficult to compute dynamic properties of the quark-gluon plasma. A conjecture made by J.M. Maldacena in 1997, called the AdS/CFT correspondence, offers a solution. The correspondence relates weakly coupled gravitational theories to strongly coupled gauge theories. Computations in weakly coupled theories are in general way easier since they can be performed using perturbation theory. The AdS/CFT correspondence makes it thus possible to determine properties of strongly coupled systems, which can not be determined using the conventional methods.

In this thesis I will show how the correspondence can be used to determine the viscosity to entropy density ratio of a strongly coupled fluid. This prediction will be compared to the experimental results on the quark-gluon plasma.

The thesis is organised as follows:

- In the first part all the necessary background theory is treated. This part consists out of chapters 2-5. Chapter 2 discusses quantum chromodynamics. In chapter 3 general relativity and black holes are discussed. Chapters 4 and 5 discuss thermo- and hydrodynamics, respectively.
- In the second part the AdS/CFT correspondence is discussed (chapter 6) and the viscosity to entropy density ratio of a strongly coupled fluid is determined using the correspondence (chapter 7).
- In the third part, chapter 8, the experiments on the quark-gluon plasma will be discussed. From these results the viscosity to entropy density ratio of the quark-gluon plasma will be determined. This value is then compared to the value predicted by the AdS/CFT correspondence.

A remark on the used conventions:
Unless stated otherwise the constants k_b, $\hbar$ and c will be set equal to 1. We will work with the mostly plus sign convention, for which the Minkowski metric is defined as: $\eta_{\mu\nu} = \text{diag}(-1, +1, +1, +1)$.

2 Quantum chromodynamics

The strong interaction is one of the four fundamental interactions, the other three are the weak interaction, the electromagnetic interaction and gravity. The strong interaction is described by the quantum field theory called quantum chromodynamics (QCD). First a short overview of QCD will be given before moving on to the technical aspects of QCD. One of the most interesting features of QCD, asymptotic freedom, will be discussed after this. The last section will shortly explain why it is difficult to do calculations on strongly coupled systems.

2.1 Basic properties of the strong interaction

QCD is a theory which describes the interaction between quarks and gluons, it is the force which binds quarks into nucleons and nucleons into atoms. QCD has the following properties:

- **Quarks** QCD describes 6 quarks and their anti-quarks. Quarks were originally conceived to explain the large amount of hadrons which collider experiments had produced. At first it was not clear if they really existed or if they were just a mathematical trick, but scattering experiments showed that quarks are real. There must be at least three quarks to explain the composition of the known hadrons. The other three quarks are necessary for theoretical reasons and to explain observations like CP violation. By now all six quarks have been observed in collider experiments. The quarks have half-integer spin and a charge of either $\frac{2}{3}$e or $-\frac{1}{3}$e. Baryons consist out of $3q$ and mesons out of a $q\bar{q}$-pair, but these are just the valence quarks which contribute only slightly to the total mass of the hadron. The valence quarks are surrounded by a polarized vacuum consisting of gluons and dynamical (virtual) quarks. These gluons and dynamical quarks give hadrons most of their mass [1].

- **Colour** Quarks have an internal degree of freedom called colour, to explain the existence of for example the $\Delta^{++}(uuu)$ hadron. This is a baryon with three equal quarks, a spin of 3/2 and an angular momentum of zero, which means that all three quarks have the same quantum numbers. But quarks are fermions, so the existence of these particles is in contradiction with Pauli's exclusion principle. To solve this problem a new degree of freedom was proposed: colour. The number of colours needed is three to explain the number of quarks in baryons and mesons. The three colours are called blue, green and red, the combination of the three colours is white/colour neutral, analogous to the real colours.

- **SU(3) gauge symmetry and gluons** The colours form a gauge group with SU(3) colour symmetry. This symmetry group has a total of 8 gauge bosons, the gluons. The gluons are the particles which mediate the strong force and bind quarks into hadrons.

- **Confinement** Isolated quarks, or isolated colour charges in general, have never been seen in nature. Quarks always form combinations in such a way that the total hadron is colour neutral. The exact mechanism of confinement is still under discussion but a necessary condition for confinement is that the theory becomes weak on small length scales and strong on large length scales. The only theories which have exactly this behaviour are the non-abelian gauge theories. How does a strong coupling cause confinement? Imagine a $q\bar{q}$ pair connected by a string. When the distance between q and $\bar{q}$ increases the energy in the string increases until it is high enough to create a new $q\bar{q}$-pair. These again form colour neutral combinations with the original pair. A quark will thus never become free, as soon as its distance to other quarks becomes to large, new quarks emerge [2].

- **Asymptotic freedom** Calculations in perturbation theory show that the effective coupling constant becomes asymptotically small for large energies. This means that quarks and gluon behave as almost free particles at these high energies.

The quark-gluon plasma

At high enough energy densities and/or temperatures quarks and gluons form a new state of matter in which they no longer belong to a single hadron. This state of matter is called the quark gluon plasma (QGP). At first it was expected that the plasma is extremely weakly coupled due to the asymptotic freedom. But experiments showed something completely different. They showed that the QGP, at the energy densities reached in these experiments, is still relatively strongly coupled

and behaves as an almost perfect fluid [3]. Theoretical considerations and experimental results of how it is known that the QGP behaves as an almost perfect fluid will be discussed in chapter 7 and chapter 8.

The QGP is studied for several reasons [4], firstly, it might give insight into the first moments after the Big Bang, which is expected to be a hot QGP. A second reason is that the QGP gives insight into how the strong interaction works at intermediate energies.

Gauge theory

As mentioned, QCD is a non-abelian gauge theory with SU(3) gauge symmetry. This section will explain what is exactly meant with this. Non-abelian means that not all the transformations belonging to the group commute ($AB \neq BA$). Due to the non-abelian nature of the theory gluons are able to interact with each other. In contrast to QED in which photons do not interact with each other [4]. A gauge theory is a theory for which the Lagrangian is invariant under certain phase transformations. As an example the theory of electromagnetism (QED) will be discussed, this is an abelian U(1) gauge theory. QED is a simpler theory to discuss than QCD because it has only one gauge boson which does not self-interact.

The Lagrangian of minimally coupled QED is given by [5]:

$$\mathcal{L}_{QED} = \bar{\psi}(i\not{D} - m)\psi - \frac{1}{4}(F_{\mu\nu})^2 \tag{2.1}$$

the field strength ($F_{\mu\nu}$) and $\not{D}$ are defined as:

$$F_{\mu\nu} = \partial_\mu A_\nu - \partial_\nu A_\mu \tag{2.2a}$$

$$\not{D} = \gamma^\mu(\partial_\mu + ieA_\mu) \tag{2.2b}$$

A_μ is the electromagnetic four-potential. The gauge transformations are defined as [6]:

$$\psi \to e^{-i\alpha}\psi \tag{2.3a}$$

$$\bar{\psi} \to e^{i\alpha}\bar{\psi} \tag{2.3b}$$

$$A_\mu \to A_\mu + \frac{1}{e}\partial_\mu\alpha \tag{2.3c}$$

It is clear that the phases cancel out due to the multiplication of ψ with $\bar{\psi}$ and that the field strength is invariant under these transformations. Thus the Lagrangian is invariant under gauge transformations. This shows that A_μ is not defined uniquely but determined up to a derivative. These formulas, valid for QED, can be generalized to the theory of QCD. This is however less straightforward than the example for QED since ψ now consists out of 6 fields, one for each colour and anti-colour. There will also be a total of eight potentials since QCD has eight gluons. It is further complicated by the gluon self-interaction. The Lagrangian of QCD is given by [7]:

$$\mathcal{L}_{QCD} = \sum_f \bar{\psi}_f(i\not{D} - m_f)\psi_f - \frac{1}{2}\mathrm{tr}(G_{\mu\nu}G^{\mu\nu}) \tag{2.4a}$$

The sum is over the 6 quark flavours and $\not{D}$ and $G_{\mu\nu}$ are given by:

$$\not{D} = \gamma^\mu(\partial_\mu - igA_\mu) \tag{2.4b}$$

Where g is the coupling constant.

$$G_{\mu\nu} = \partial_\mu A_\nu - \partial_\nu A_\mu - ig[A_\mu, A_\nu] \tag{2.4c}$$

The extra term, in comparison with QED, stems from the non-abelian nature of QCD and couples gluons to each other. A_μ is a combination of the eight separate gluons and is given by:

$$A_\mu = \sum_{a=1}^{8} A_\mu^a \lambda^a/2 \tag{2.4d}$$

λ^a are the eight Gell-Mann matrices, which is a representation of the SU(3) group. Also in this case the Lagrangian is invariant under certain gauge transformations.

Energy dependence of the coupling constant

As explained QCD has a coupling constant which increases when the energy scale decreases, whereas QED has a coupling constant which has the opposite behaviour. Most theories have effective coupling constants that depend on the energy scale. An exception is the class of conformal field theories (CFTs) which has a coupling constant independent of energy. This means that CFTs are invariant under rescaling. Figure 1 gives a schematic overview of how the coupling constant depends on the energy for the different theories, it also shows the schematic position of the systems which will be discussed in the other chapters.

A consequence of the opposite scaling behaviour of the QED and QCD coupling constants is the fact that we can imagine an energy scale where all forces have the same coupling strength. At energies we are accustomed to the strong force is stronger than the electromagnetic force but as the energy increases the strong force will become weaker whereas the electromagnetic force will become stronger. The coupling constants will thus eventually become of comparable size. This is the basis of grand unified theories, which try to unify all fundamental interactions [8].

How can the energy dependence of the coupling constant be explained? In the case of QED there is an easy conceptual explanation called screening. We imagine the electron to have an infinite bare charge surrounded by virtual electron/positron pairs. At large distances the infinite electron charge is screened by the pairs resulting in an effective charge of e [7]. The closer a particle gets to the electron the lesser its charge is screened. This means that the effective coupling constant will increase at small distances (high energies).

In the case of QCD it is a bit more difficult. The virtual $q\bar{q}$ pairs screen the charge, equivalent to screening in QED, whereas the virtual gluons cause anti-screening. The net effect will be an anti-screened charge. This results in an interaction strength which becomes extremely small for high energies [8].

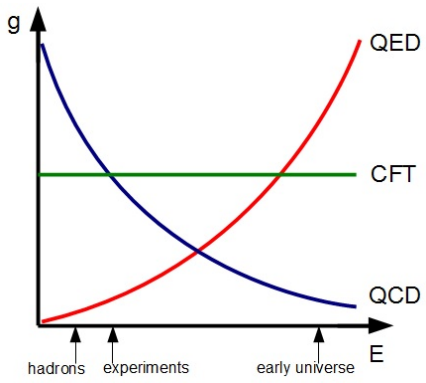

Figure 1: Energy dependence of coupling strength

β-function

The arguments mentioned above can be made more exact using the β-function, which is a mathematical function that describes the energy dependence of the coupling constant [5]. It is defined as:

$$\beta(\lambda) = M\frac{\partial\lambda}{\partial M} \tag{2.5}$$

with λ the effective coupling constant and M the energy scale. The β-function is determined using a perturbative approach by expanding it into powers of the coupling constant. The first order term of the β-function is called the one-loop β-function, which takes into account only the Feynman diagrams with just one loop. Due to this approximation it is only valid for small coupling constants. The one-loop β-function can be negative positive or zero. An example of a theory with a positive β-function is QED, the coupling increases for increasing energy. QCD is a theory with a negative β-function, which means that the coupling constant decreases for increasing energy. This shows that the theory of QCD has asymptotic freedom. Conformal field theories have a β-function which is exactly zero, the interaction strength is independent of the energy scale.

2.2 Doing calculations on a strongly coupled system

It is extremely difficult to do calculations on a strongly coupled system, for example the quark-gluon plasma, because it is not possible to use perturbation theory, which only works for a small coupling constant. Perturbation theory unfortunately breaks down for large coupling constant. Another problem with perturbation theory, besides the strong coupling, is that at high energies lots of gluons and quark/anti-quark pairs are produced. This increases the number of degrees of freedom drastically, which also causes perturbation theory to break down [9]. Techniques to do calculations on strongly coupled systems have been developed, the most frequently used technique is lattice gauge theory. Lattice QCD uses a discrete version of QCD where everything is defined on a lattice. Lattice theory works best for static problems, for example calculating the mass of the proton, which can be determined reasonably accurate using lattice theory. Other properties which can be studied using lattice QCD are the equation of state, energy density and pressure [10]. But lattice theory has its limits, for dynamic, time dependent problems it is difficult to relate lattice calculations to the observables [11]. This makes it difficult to determine transport properties, like the viscosity, using lattice QCD. In recent years physicists have been looking at the AdS/CFT correspondence as a tool to calculate properties of strongly coupled systems. The correspondence and how it can be used will be discussed in subsequent chapters.

3 Black holes

Black holes are solutions of the Einstein equations. They are objects which are so compact and heavy that nothing can escape the vicinity of the object. Even light is unable to escape if it gets to close, thus the name 'black hole'. In order to understand black holes the following sections will first discuss the basics of general relativity, before moving on to the Schwarzschild black hole. After this the anti-de Sitter spacetime and the AdS-Schwarzschild black hole will discussed. The last section will be on surface gravity, what it is and how to calculate it. The books 'General Relativity' by R.M.Wald [12] and 'An introduction to black holes, information and the String theory revolution' by L.Susskind and J. Lindesay [13] were used to write this chapter.

3.1 General relativity and the Einstein equations

Before general relativity, special relativity was established. Special relativity is concerned with objects which move at high velocities, whereas general relativity determines what happens to objects and spacetime when gravity is put in. In special relativity spacetime is flat and the metric is given by the Minkowski metric: $\eta_{\mu\nu} = \text{diag}(-1, +1, +1, +1)$. In general relativity spacetime itself is deformed in the presence of mass/energy and it is thus no longer flat. The effect of mass on spacetime is given by the Einstein equations:

$$R_{\mu\nu} - \frac{1}{2}Rg_{\mu\nu} + \Lambda g_{\mu\nu} = 8\pi G T_{\mu\nu} \tag{3.1}$$

here $T_{\mu\nu}$ is the energy-momentum tensor, $R_{\mu\nu}$ is the Ricci tensor, $g_{\mu\nu}$ is the metric, R is the scalar curvature and Λ is called the cosmological constant. A positive Λ accelerates the expansion of the universe whereas a negative Λ decelerates the expansion of the universe. The Ricci tensor and the scalar curvature are defined by the Christoffel symbols and the Riemann tensor. The Christoffel symbols describe the effect of curved spacetime on vectors. Mathematically they are used to construct a covariant derivative of a vector ($\nabla_\mu V^\nu$) which transforms as tensor whereas the partial derivative of a vector ($\partial_\mu V^\nu$) in general doesn't transform as a tensor [14].

$$\nabla_\mu V^\nu = \partial_\mu V^\nu + V^\alpha \Gamma^\nu_{\alpha\mu} \tag{3.2}$$

The Christoffel symbols are defined as:

$$\Gamma^i_{kl} = \frac{1}{2}g^{im}\left(\frac{\partial g_{mk}}{\partial x^l} + \frac{\partial g_{ml}}{\partial x^k} - \frac{\partial g_{kl}}{\partial x^m}\right) \tag{3.3a}$$

The Christoffel symbols are thus related to the metric and its derivatives. The Riemann tensor is defined as:

$$R^\alpha_{\mu\nu\rho} = \partial_\nu \Gamma^\alpha_{\mu\rho} - \partial_\rho \Gamma^\alpha_{\mu\nu} + \Gamma^\alpha_{\sigma\nu}\Gamma^\sigma_{\mu\rho} - \Gamma^\alpha_{\sigma\rho}\Gamma^\sigma_{\mu\nu} \tag{3.3b}$$

So the Riemann tensor is related to the second derivative of the metric, which makes the Einstein equations second order differential equations. The Riemann tensor is related to the curvature of spacetime: $R^\alpha_{\mu\nu\rho} = 0$ if and only if spacetime is flat (Minkowski). Curvature is an intrinsic property of a spacetime not just an artefact from the choice of coordinate system. Using the definitions for the Riemann tensor and the Christoffel symbols, the Ricci tensor and the curvature scalar are defined as:

$$R_{\mu\nu} = R^\alpha_{\mu\alpha\nu} \tag{3.4a}$$

$$R = g^{\mu\nu}R_{\mu\nu} \tag{3.4b}$$

Comparing the above definitions with the Einstein equations we see that the LHS is just related to the metric and its derivatives whereas the RHS is related to the mass and energy distribution in the universe. So mass and energy deform spacetime, this deformation is what makes planets orbit around massive objects like the sun.

In this thesis only some solutions of the Einstein equations will be discussed. All solutions discussed have $T^{\mu\nu} = 0$, which are called the vacuum solutions. Examples are the well-known flat Minkowski spacetime and the Schwarzschild metric (both have $\Lambda = 0$). The anti-de Sitter spacetime (AdS), which has a negative cosmological constant, and black holes in it will also be discussed. A spacetime with a positive cosmological constant is called a de Sitter spacetime, this spacetime will not be discussed here.

3.2 The Schwarzschild Black Hole

The Schwarzschild metric is the vacuum solution of the Einstein equations, without cosmological constant. It determines how a massive object deforms the empty spacetime surrounding it. We consider a spherically symmetric, static mass without charge. With these conditions and the assumption that the solution must reduce to Newtonian mechanics in the classical limit (weak field and low velocities), the Schwarzschild metric is determined uniquely:

$$ds^2 = -\left(1 - \frac{2MG}{r}\right) dt^2 + \left(1 - \frac{2MG}{r}\right)^{-1} dr^2 + r^2 d\Omega^2 \tag{3.5}$$

it is only valid outside the massive object. We see that the solution is static and spherically symmetric since the metric doesn't depend on time or any of the angles. It is also evident that the metric reduces to the Minkowski metric when an observer is far away from the black hole ($r \to \infty$) or when the black hole mass approaches zero.

The metric has two singularities one at $r = 2MG$ and one at $r = 0$. The singularity at $r = 0$ is a real singularity where the laws of physics break down. The other singularity, at $r = 2MG$ is called the Schwarzschild radius or horizon, this singularity is just a coordinate singularity. When an object falls towards a black hole it does not notice the moment it passes the horizon, the laws of physics are exactly the same. This shows that the singularity at the horizon is just an artefact from the choice of coordinates. Even though the horizon is not a real singularity it is special since it is a point of no return. Once the horizon is passed the object can never leave the black hole and it must necessarily fall towards the centre. This can be represented by figure 2.

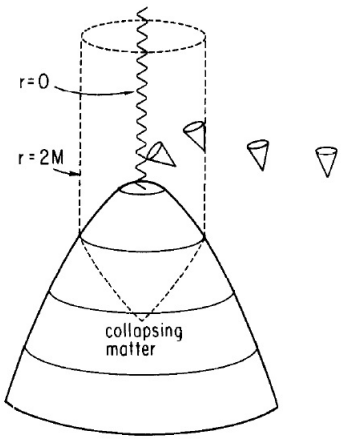

Figure 2: Tipping of the light cone in the gravitational field of a black hole, $G = 1$ [12]

The dotted line represents the position of the horizon. Light cones which get closer to the black hole start to tip due to the increasing curvature of spacetime. Light cones represent all possible paths which a particle can follow, never faster than with the speed of light. A massless particle will move exactly on the light cone, a massive particles must follow world lines which lie inside the cone. The figure shows that for a massive particle at the horizon its motion is inevitably towards the black hole, because the forward light cone at the horizon is directed completely towards the centre of the black hole.

Another way to see that particles cannot escape a black hole once they are inside the horizon is that the metric switches sign when the horizon is reached: $1 - \frac{2MG}{r}$ is positive outside the horizon but negative inside the horizon. This switch can be considered as a switch of the time-like coordinate with the space-like coordinate. But you can never move backwards in time, after the horizon is reached this changes to not being able to move backwards in space. So a particle inevitably moves towards the centre of the black hole after it has crossed the horizon.

The Schwarzschild radius doesn't matter in most cases since most objects are not dense enough to have a horizon outside the object. For comparison the Schwarzschild radius of an object with the mass of the sun is just 3 km (radius of sun is 695.800 km). So the horizon singularity is only relevant for extremely massive and compact objects, called black holes. Black holes are created when a massive star (about 10 times the solar mass) collapses at the end of its lifetime.

3.3 AdS spacetime and the AdS-Schwarzschild black hole

Anti-de Sitter spacetime is the vacuum solution of the Einstein equations with a negative cosmological constant, which means that it has a negative curvature. The metric for AdS_5 is most conveniently written in Poincaré coordinates and can be written as

$$ds^2 = \frac{r^2}{L^2}(-dt^2 + dx_i^2) + \frac{L^2}{r^2}dr^2); \quad i = 1, 2, 3 \tag{3.6a}$$

or

$$ds^2 = \frac{L^2}{z^2}(-dt^2 + dx_i^2 + dz^2); \quad i = 1, 2, 3 \tag{3.6b}$$

z is called the holographic dimension and is defined as $z = L^2/r$, L is the curvature radius of the AdS spacetime. From the metric it can be seen that this spacetime has a boundary at $z = 0$, $r \to \infty$. This boundary will be important when the AdS/CFT correspondence is discussed. Analogously to the Schwarzschild metric for flat spacetime we can define a metric which determines how empty AdS spacetime is curved in the vicinity of a massive object. The metric for the AdS_5-Schwarzschild black hole is given by:

$$ds^2 = \frac{r^2}{L^2}\left(-f(r)dt^2 + dx_i^2\right) + \frac{L^2}{r^2}\frac{1}{f(r)}dr^2; \quad i = 1, 2, 3; \quad f(r) = 1 - \frac{r_0^4}{r^4} \tag{3.7a}$$

or

$$ds^2 = \frac{L^2}{z^2}\left(-f(z)dt^2 + dx_i^2 + \frac{1}{f(z)}dz^2\right); \quad i = 1, 2, 3; \quad f(z) = 1 - \frac{z^4}{z_0^4} \tag{3.7b}$$

Just as the Schwarzschild metric reduces to flat spacetime this metric reduces to the AdS metric for $z \to 0$, $r \to \infty$. This metric has a horizon at $z = z_0$.

3.4 Surface gravity

The surface gravity is defined as the acceleration of a particle at the horizon, as measured by an observer at infinity. The proper acceleration felt by the in-falling particle will be infinite but due to gravitational redshift the acceleration measured by an observer at infinity is finite. For a general metric $ds^2 = -f(r)dt^2 + \frac{dr^2}{f(r)}$ the surface gravity is given by [14]:

$$\kappa = \frac{f'(r_0)}{2} \tag{3.8}$$

where the derivative is with respect to r. This formula can be used to determine the surface gravity of the Schwarzschild and AdS-Schwarzschild black hole. For the metric of the Schwarzschild black hole given in equation (3.5) $f(r) = 1 - \frac{2MG}{r}$, putting this into equation (3.8) gives:

$$\kappa_{S-BH} = \frac{1}{4MG} \tag{3.9a}$$

Which is exactly what you would expect by comparing Newtons second law with his law of universal gravitation at $r = r_0 = 2MG$: $\frac{mMG}{r_0^2} = m\kappa \to \kappa = \frac{1}{4MG}$. For an AdS-Schwarzschild black hole $f(r) = \frac{r^2}{L^2}\left(1 - \frac{r_0^4}{r^4}\right)$. This gives

$$\kappa_{AdS-S-BH} = \frac{2r_0}{L^2} \tag{3.9b}$$

4 Thermodynamics

In this chapter first some general remarks about thermodynamics will be made before discussing the thermodynamic properties (e.g. entropy) of black holes. Thereafter the temperature of the Schwarzschild and AdS-Schwarzschild black hole will be determined from the thermodynamic laws. In the last two sections a faster method for deriving the temperature of these black holes will be discussed and an alternative way to derive the entropy law will be shown.

4.1 Thermodynamic relations

Some relevant thermodynamic formulas relating the pressure, temperature and entropy of a fluid are [15]:

$$d\epsilon = Tds \tag{4.1a}$$

ϵ is the internal energy density, T the temperature and s the entropy density. The pressure is

$$dp = sdT \tag{4.1b}$$

These two equations together give

$$\epsilon + p = Ts \tag{4.1c}$$

these equations assume a constant volume and number of particles. It is also assumed that the baryon chemical potential is zero.

Conformal fluids

The energy momentum tensor of conformal fluids must obey the condition $T^\mu_\mu = 0$. We will not derive this here but just give a plausible explanation by looking at the equation of state of a photon gas. A photon gas is a conformal fluid because photons are massless and thus scale invariant (which usually implies conformal invariance). The photon gas has equation of state $\epsilon = 3p$. Assuming that a photon gas is close to a perfect gas, since photons have almost no interaction this is a realistic assumption, the energy momentum tensor and its trace is defined as

$$T^{\mu\nu} = \text{diag}(\epsilon, p, p, p) \rightarrow T^\mu_\mu = \eta_{\mu\nu}T^{\mu\nu} = -\epsilon + 3p \tag{4.2}$$

This implies that for conformal fluids the equation of state can be determined by imposing the condition $T^\mu_\mu = 0$. Conformal fluids in 3+1 dimensions have $\epsilon = 3p$ as equation of state.

4.2 Black hole thermodynamics

Black hole laws are very similar to the thermodynamic laws. One of these, the fact that the area of a black hole never decreases can be related to the second law of thermodynamics: *'The entropy of a closed system never decreases'*. From this similarity Bekenstein proposed [16] that black holes have some sort of intrinsic entropy, which depends on the area of the black hole horizon. When an object falls into a black hole the total entropy decreases, but this can never happen according to the second law of thermodynamics. By assigning entropy to the area of black hole this problem is solved, since the area and thus the entropy of a black hole increases when matter falls in. The thermodynamic and black hole laws are summarized in table 1.

	Thermodynamics	Black holes
0^{th}	T constant for system in equilibrium	κ constant on black hole surface
1^{st}	$\delta E = T\delta S$	$\delta M = \frac{\kappa}{8\pi G}\delta A$
2^{nd}	$\delta S \geq 0$	$\delta A \geq 0$
3^{rd}	$T \neq 0$	$\kappa \neq 0$

Table 1: Comparison of black hole laws with thermodynamics [17]

κ is the surface gravity at the black hole horizon, it is determined by equation (3.8). Note that the Schwarzschild black hole is stationary so its energy is just its mass; $\delta E = \delta M$.

The 1st black hole law can be derived by considering a Schwarzschild black hole. The area of the horizon is given by $A = 4\pi r_0^2 = 16\pi(MG)^2$. Taking the derivative with respect to M gives: $\delta A = 32\pi MG^2\delta M$. Since the surface gravity of a Schwarzschild black hole is given by $\kappa = \frac{1}{4MG}$ we get $\delta M = \frac{\kappa}{8\pi G}\delta A$ [14]. From the comparison of these laws the following relations between thermodynamics and black hole variables can be made [17]:

$$T = \epsilon\kappa \tag{4.3a}$$

$$S = \eta A \tag{4.3b}$$

Both ϵ and η are dimensionless constants and are related by:

$$\epsilon\eta 8\pi G = 1 \tag{4.3c}$$

For this comparison to be possible black holes have to have a temperature. When Bekenstein proposed his idea the general opinion was that black holes can not emit radiation and thus have a temperature which is absolute zero. Later Hawking [18] showed that when quantum mechanical effects are included black holes do emit radiation, as if they are thermal bodies with a temperature of $T = \frac{\kappa}{2\pi}$. From this relation and equation (4.3) the entropy law can be determined [17]:

$$S = \frac{A}{4G} \tag{4.4}$$

This allows us to determine the entropy of a Schwarzschild black hole, since the area of the horizon is given by $A = 4\pi r_0^2$ with $r_0 = 2MG$ the entropy is $S_{Schwarzschild} = 4\pi M^2 G$.

Even though the entropy law for black holes is derived for the Schwarzschild black hole this law is valid for all black holes, including the AdS-Schwarzschild black hole.

How can a black hole emit radiation?

Since nothing can come out of the volume enclosed by the event horizon we would naively expect that it is not possible for a black hole to lose mass. Classically this idea is valid but when quantum mechanics is taken into account a black hole is able to lose mass. This goes as follows, in quantum mechanics the vacuum is not really empty but is filled with pairs of virtual particles. These pairs consist out of a particle with positive energy and an (anti-)particle with negative energy. When such a virtual pair is created close to the black hole horizon it is possible that the particle escapes whereas the antiparticle with negative energy tunnels into the black hole. Effectively the black hole loses energy whereas it 'emits' radiation in the form of the escaping particle. This radiation can be related to the temperature of a black hole [19].

4.3 Deriving the temperature of black holes from thermodynamics

The Hawking temperature is given by:

$$T = \frac{\kappa}{2\pi} \tag{4.5}$$

This is the temperature as measured by an observer at infinity. The temperatures of the Schwarzschild and AdS-Schwarzschild black hole can be determined using equation (3.9), which gives the surface gravity of the two black holes.

$$T_{S-BH} = \frac{\kappa}{2\pi} = \frac{1}{8\pi MG} \tag{4.6a}$$

$$T_{AdS-S-BH} = \frac{\kappa}{2\pi} = \frac{r_0}{\pi L^2} = \frac{1}{\pi z_0} \tag{4.6b}$$

We see from the first equation that the temperature of a Schwarzschild black hole is inversely proportional to its mass. This means that a heavy Schwarzschild black hole has a lower temperature and thus emits radiation slower than a smaller Schwarzschild black hole. This relation will make a Schwarzschild black hole unstable in the following way, when a black hole radiates it loses energy which will decreases its mass but increase its temperature. This will make it radiate even faster until the black hole has evaporated completely. A black hole can become stable when it is put in AdS spacetime instead of flat spacetime [20]. This can be shown by looking at the second equation, which shows that the temperature of an AdS-Schwarzschild black hole is proportional to the radius of the horizon. Since the horizon always increases when mass falls into a black hole, the temperature also increases when the mass increases. An AdS-Schwarzschild black hole is thus thermodynamically stable, since its temperature goes down when it emits radiation.

4.4 Deriving the temperature of black holes using a Wick rotation

Black holes have a coordinate singularity at the horizon r_0. Since this is just a coordinate singularity is should be possible to change coordinates in such a way that the singularity is removed. Doing this in a specific way will result in a metric which can be used to determine the temperature of a black hole. A first step to remove the singularity is to do a Wick rotation. Before moving on, it will first be explained what this is and how it is related to the temperature.

Wick rotation

A Wick rotation is defined as $t \to -i\tau$. It basically assumes that time can also take imaginary values and then rotates the real time axis by 90 degrees onto the imaginary axis. Looking at the Minkowski metric we see it does the following:

$$ds^2 = -dt^2 + dx_i^2 \to ds^2 = d\tau^2 + dx_i^2 \tag{4.7}$$

The timelike coordinate is changed to a spacelike coordinate. The metric is changed from Lorentzian to Euclidean signature. A Wick rotation is needed to relate the quantum mechanical time evolution operator with the partition function from statistical mechanics. This goes as follows:
The partition function is:

$$Z = \sum_i e^{-\beta E_i} = \sum_n \langle n|e^{-\beta \hat{H}}|n\rangle; \quad \beta = \frac{1}{T} \tag{4.8}$$

The last step follows from the fact that we can always chose a basis such that E_i are the eigenvalues of the operator $\hat{H}$.
The time evolution operator in quantum mechanics is:

$$A = \langle x|e^{-i\Delta t \hat{H}}|x'\rangle \tag{4.9a}$$

It is the amplitude to go from $x \to x'$ in time Δt. If we want to know the amplitude to go from x back to x in a time Δt, with every possible state in between, this changes to

$$A = \sum_{\text{all paths}} \langle x|e^{-i\Delta t \hat{H}}|x\rangle \tag{4.9b}$$

If we do a Wick rotation ($t \to -i\tau$) on (4.9b) the equation changes to:

$$A = \sum_{\text{all paths}} \langle x|e^{-\Delta \tau \hat{H}}|x\rangle \tag{4.9c}$$

Next we compactify the euclidean time by imposing a periodicity condition on τ: $\tau + \Delta\tau = \tau$. Graphically this can be explained as follows, imagine a piece of paper as a two dimensional euclidean space. The horizontal direction is the spatial direction and the vertical direction the euclidean time. The periodicity condition is equivalent to rolling up the vertical direction in order to get a cylinder. This last trick allows us to compare the partition function from statistical mechanics with this Wick rotated operator. If we identify β as the period of τ the partition function and the operator are equal:

$$\Delta\tau = \beta = \frac{1}{T} \tag{4.10}$$

The periodicity of the euclidean (wick rotated) time, or 'circumference' of the compactified time coordinate, can thus be identified with the inverse temperature. This identification can be used to determine the temperature of some black holes. The next sections will first show how this is done for the Schwarzschild and AdS-Schwarzschild black hole, before giving the general method.

Temperature of a Schwarzschild black hole

The metric of the Schwarzschild black hole (3.5) is:

$$ds^2 = -(1 - \frac{2MG}{r})dt^2 + (1 - \frac{2MG}{r})^{-1}dr^2 + r^2 d\Omega^2 \tag{4.11a}$$

First the Wick rotation will be performed

$$ds^2 = (1 - \frac{2MG}{r})d\tau^2 + (1 - \frac{2MG}{r})^{-1}dr^2 + r^2 d\Omega^2 \tag{4.11b}$$

In order to look a the metric near (just outside) the horizon we will do an expansion around $r_0 = 2MG$, $r = r_0 + \epsilon$ with $\epsilon \ll 1$, to first order we obtain:

$$ds^2 = \frac{\epsilon}{2MG}d\tau^2 + \frac{2M}{\epsilon}d\epsilon^2 + (2MG)^2 d\Omega^2 \tag{4.11c}$$

From now on we the last term will be omitted since this is just a constant. Doing the following coordinate transformations; $\epsilon = x^2$, $x = \frac{\rho}{\sqrt{8MG}}$ and $\tau = 4MG\theta$ the metric becomes:

$$ds^2 = \rho^2 d\theta^2 + d\rho^2 \tag{4.11d}$$

This is precisely the metric of 2D flat space in polar coordinates. At first sight it might look like the singularity at $r = 2MG$ has disappeared, but we should be a bit more careful with this statement. The singularity has disappeared only if θ is periodic: $\theta = \theta + 2\pi$, otherwise the space will not be flat but form a cone, which will result in a conical singularity at the horizon.

A conical singularity can be represented graphically in the following way : Imagine a circle on a piece of paper (see figure 3) and draw a point in the middle which is identified with the horizon. As long as the circle is complete this paper is flat. Now a piece is taken out of the circle, in order to put the sides together the paper has to form a cone, with a singularity at its tip (thus the name *conical* singularity). So $\theta = \theta + 2\pi$ in order to have a metric for which the singularity at the horizon has disappeared.

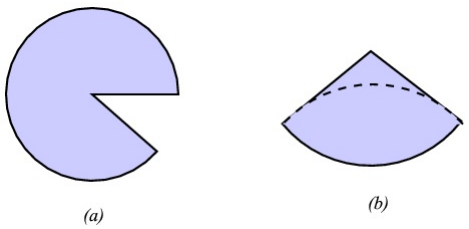

Figure 3: Flat space forms a cone when θ has a periodicity smaller than 2π [21]

What does this condition mean for τ? Since $\tau = 4MG\theta$ the periodicity condition on θ also imposes a periodicity condition on τ:

$$\theta = \theta + 2\pi \rightarrow \tau = \tau + 8\pi MG \tag{4.12}$$

So τ has a period of $8\pi MG$. It is now possible to define the temperature of the black hole using equation (4.10). We obtain: $T = \frac{1}{8\pi MG}$, which is exactly the same as the temperature of the Schwarzschild black hole we derived earlier.

Temperature of an AdS-Schwarzschild black hole

The exact same method can be used to derive the temperature of an AdS-Schwarzschild black hole. Starting with the metric (3.7a):

$$ds^2 = \frac{L^2}{z^2}\left(-f(z)dt^2 + dx_i^2 + \frac{1}{f(z)}dz^2\right); i = 1, 2, 3 \tag{4.13}$$

The first step is again a Wick rotation $t = -i\tau$. Secondly we will look at the metric just outside the horizon. Since z runs from z_0 to 0 we have to take $z = z_0 - \epsilon$ instead of $z = z_0 + \epsilon$. The x_i part of the metric will be ignored since it is constant. We obtain the metric:

$$ds^2 = \frac{L^2}{z_0^2}\left(\frac{4\epsilon}{z_0}d\tau^2 + \frac{z_0}{4\epsilon}d\epsilon^2\right) \tag{4.14a}$$

Thereafter the following coordinate transformations are done $\epsilon = x^2$, $\rho = \frac{L}{\sqrt{z_0}}x$ and $\theta = \frac{2}{z_0}\tau$ to end up again with the metric of a 2D flat space in polar coordinates

$$ds^2 = \rho^2 d\theta^2 + d\rho^2 \tag{4.14b}$$

Looking back at the transformations it is clear that the period of τ is equal to πz_0. We obtain $T = \frac{1}{\pi z_0}$ as the temperature of the AdS-Schwarzschild black hole. Which is again equal to the temperature derived in the previous section.

General method to determine temperature

As we can see from the two examples shown there is a general method to determine the temperature of a black hole. The method is a follows:

- Perform a Wick rotation
- Look at metric just outside of the horizon $r = r_0 + \epsilon$, $\epsilon \ll 1$ and keep terms to smallest order in ϵ
- Omit the terms which are constant
- Change coordinates in such a way that you end up with the metric of 2D flat space in polar coordinates
- Determine periodicity of τ from periodic condition on θ
- Since the periodicity of τ is related to β, which is the inverse of the temperature, this will give the temperature of the black hole

4.5 Deriving the entropy law from the black hole temperature

It is possible to derive the entropy law directly from the temperature of the Schwarzschild black hole using $dE = TdS$ [13]. E and S are now the total energy and entropy instead of the densities which were used in equation (4.1a). Since the Schwarzschild black hole is stationary the energy of the black hole is equal to the black hole mass, $E = M$. Integrating the differential equation, using $T = \frac{1}{8\pi GM}$, we obtain: $S = 4\pi GM^2$. We do not put in an integration constant since the entropy goes to zero when the mass goes to zero. Since the area is given by $A = 4\pi r_0^2 = 16\pi(MG)^2$ we obtain $S = \frac{A}{4G}$. Which is equal to the entropy law derived earlier.

5 Hydrodynamics

Hydrodynamics - or more appropriately fluid dynamics - describes the behaviour of gases and liquids in motion. Hydrodynamics is used to calculate the bulk properties, like pressure. It allows us to neglect the discrete molecular structure of a fluid. This means that it can only be used when the mean free path of the particles is much smaller than the size of the system: $\lambda << L$ [15] [22]. We will first look at the hydrodynamic equations and then explain what viscosity is. This chapter was written using the book 'Fluid Dynamics' by P.K. Kundu et al. [22].

5.1 The Navier-Stokes equations and the energy-momentum tensor

The Navier-Stokes equations describe the behaviour of a fluid. The equations are a statement of how the mass and momentum in the system are conserved without dissipative effects or how they change when dissipative effects like viscosity are included. The Navier-Stokes equations can be written in both a non-relativistic and a relativistic form. To describe the QGP the relativistic Navier-Stokes are needed but since these are more complicated the non-relativistic equations will be discussed first.

Non-relativistic

The non-relativistic Navier-Stokes equation for an incompressible fluid is given by:

$$\rho\left[\frac{\partial\vec{u}}{\partial t}+(\vec{u}\cdot\vec{\nabla})\vec{u}\right]=\rho\vec{g}-\vec{\nabla}p+\eta\nabla^2\vec{u} \tag{5.1}$$

ρ is the density, $\vec{u}$ is the velocity, p is the pressure, $\vec{g}$ is the external force and η is the shear viscosity. The first term on the LHS describes the change of momentum due to changes in the velocity field, the second describes the convection. The first term on RHS is the external source, the second term describes how particle move due to pressure differences and the third and last term is the diffusion, the way particles affect each other. This last term is the term we are most interested in since it contains η, which is the shear viscosity. A perfect fluid is a fluid which has no viscosity ($\eta = 0$) as well as being incompressible. These equations can be derived by imposing mass and momentum conservation on the system. A short overview of the derivation is given in appendix A.

Relativistic

The relativistic Navier-Stokes equation is: $\partial_\mu T^{\mu\nu} = 0$. $T^{\mu\nu}$ is the energy-momentum tensor, it depends on the kind of fluid that is described. First we will look at $T^{\mu\nu}$ for a perfect fluid. In a perfect fluid the particles do not interact with each other, which means that there are no dissipative effects. In this case $T^{\mu\nu}$ is given by:

$$T^{\mu\nu}=(\epsilon+p)u^\mu u^\nu+pg^{\mu\nu} \tag{5.2}$$

ϵ is the mass-energy density, p is the pressure and u^μ is the four velocity defined as $u^\mu u_\mu = -1$. When we take spacetime to be flat and the fluid stationary with respect to our frame of reference ($u^\mu = (1, 0, 0, 0)$), this tensor takes the following form: $T^{\mu\nu} = \text{diag}(\epsilon, p, p, p)$ [15]. In reality the particles in a fluid always have some interaction with each other. These interactions are taken into account, to first order in derivatives, by adding $-\sigma^{\mu\nu}$ to equation (5.2). How $\sigma^{\mu\nu}$ is defined depends on the chosen reference frame, because there is some freedom in the definition for u^μ. Here the Landau frame is chosen, in which u^μ is defined as the velocity of the *energy* flow, $T^{\mu\nu}u_\mu = 0$. In the local rest frame $u^i = 0$ it is possible to chose $\sigma^{00} = \sigma^{0i} = 0$ [23]. σ^{ij} (in flat space time) is given by:

$$\sigma_{ij}=\eta(\partial_i u_j+\partial_j u_i-\frac{2}{3}\delta_{ij}\partial_k u^k)+\zeta\delta_{ij}\partial_k u^k \tag{5.3a}$$

In a general reference frame, with general metric $\sigma^{\mu\nu}$ is given by:

$$\sigma^{\mu\nu}=P^{\mu\alpha}P^{\nu\beta}\left[\eta(\nabla_\alpha u_\beta+\nabla_\beta u_\alpha)+\left(\zeta-\frac{2}{3}\eta\right)g_{\alpha\beta}\nabla\cdot u\right] \tag{5.3b}$$

ζ is the bulk viscosity. $P^{\mu\nu}$ is an operator which projects a vector onto a direction perpendicular to u^μ:

$$P^{\mu\nu} = g^{\mu\nu} + u^\mu u^\nu \tag{5.3c}$$

The definition of ∇_μ is given in equation (3.2). The formulas stated above are from [24] [25].

5.2 Viscosity

In everyday life viscosity is represented by how thick or sticky a fluid is, intuitively we understand that syrup has a higher viscosity than water. Since this intuitive idea is not applicable to all fluids, a more precise definition will be given. There are two kinds of viscosity, shear and bulk viscosity. Bulk viscosity describes how a fluid reacts when it is compressed or stretched, it becomes important when for example sound waves are considered [3]. Since the bulk viscosity is usually a lot smaller than the shear viscosity, or even zero when the fluid is incompressible, it will be neglected in the coming chapters. Shear viscosity is the reaction of a fluid to shear stress, which is a force parallel to the surface. Imagine a fluid between two plates - a stationary and a moving plate - due to the relative movement of the plates a velocity gradient will arise. This velocity gradient will result in transverse momentum flow, slower layers will gain momentum and move faster whereas the layers with higher speed lose momentum. How much momentum will be transferred between the layers depends on the shear viscosity. If it is low the momentum transfer is small, whereas a high shear viscosity will result in a large momentum transfer. Figure 4 shows how shear viscosity and the resulting momentum flow changes the velocity profile from the solid line to the dashed line.

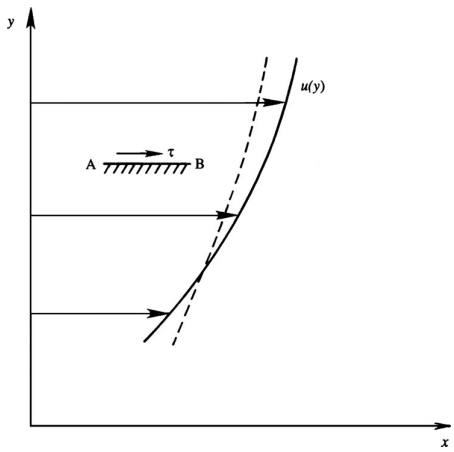

Figure 4: Shear viscosity [22]

For a 2D fluid moving in the x-direction the shear viscosity (η) is defined as:

$$\frac{F}{A} = \tau = \eta \frac{\partial v_x}{\partial y} \tag{5.4}$$

τ is the shear stress (force parallel to surface, per area). u the velocity field and y the transverse distance.

The viscosity is strongly temperature dependent. For a gas the viscosity increases with increasing temperature whereas the viscosity of a liquid decreases with increasing temperature. The reason for this completely opposite behaviour can be found in the way momentum is transferred in gases and liquids. In a gas molecules are basically free except for the occasional collisions with other molecules. Therefore the momentum transfer is mainly due to molecular diffusion (motion of individual molecules) and subsequent collisions between molecules. When the temperature is increased the molecules will start to move faster which results in more collisions, more momentum transfer and thus a higher viscosity. For a liquid the cohesive forces between molecules are the main cause of momentum flow. When the temperature gets higher the cohesive forces go down which will result in a smaller viscosity [22] [26].

The behaviour of a relativistic fluid is described by the viscosity to entropy density ratio: η/s. Since this is a dimensionless quantity it is more useful in quantifying how perfect a fluid is than the viscosity itself [26]. A perfect fluid is a fluid with $\eta/s = 0$.

Interaction strength

What does it say about the interaction strength when η/s is extremely small? To determine this let us first look at the viscosity of a weakly coupled plasma, since it is weakly coupled it can be determined using perturbation theory. It is given by [27]:

$$\eta \sim \frac{N_c^2 T^3}{(g^2 N_c)^2 ln(1/(g^2 N_c))} \tag{5.5}$$

Since the entropy of a plasma is $\propto N_c^2 T^3$, η/s depends on the coupling constant as

$$\eta/s \sim \frac{1}{g^4 ln(1/g^2)} \tag{5.6}$$

were we have omitted the dependence on N_c. This shows that the shear viscosity, as well as η/s, blows up when $g \to 0$. The shear viscosity of a non-interacting system is thus infinite. At first glance it might seem to be a bit strange that this is the case. The solution [25] here is that in systems which have such a small interaction strength hydrodynamics is not valid any more, since the mean free path is larger than the system size (remember that hydrodynamics is only valid for $\lambda << L$). In order to measure a viscosity at such a small interaction strength we would need to increase the system size. Viscosity increases for smaller interaction strength because the mean free path increases which makes it easier for a particle to diffuse into other regions [25]. The perfect gas, which does not have any interaction, has an infinite viscosity.

We come to the conclusion that weak coupling inevitably leads to large η/s. This also means that systems with a small η/s have to be strongly coupled. The reverse of these statements is not true in general [26], a strongly coupled system can have a small as well as a large viscosity.

6 AdS/CFT correspondence

All the preliminary theory has been discussed, so now we are able to discuss the AdS/CFT correspondence. The correspondence states that a $d+1$-dimensional gravity theory is dual to a d-dimensional gauge theory which lives on its boundary. It is an example of the holographic principle. But how can a theory which has less dimensions contain the same information? One hint that this is possible can be found in the entropy law for black holes. Entropy is a measure of the number of micro-states of a system, this usually scales with the volume. But the black hole entropy scales with the area, which means that all the information of the bulk can be stored on its boundary [12]. There are many forms of the duality, we will discuss the one originally proposed by Maldacena [28]. The duality itself has never been proven but performed tests have not been able to disprove it, see for example [20] for a list of tests which have been performed to check the correspondence.

6.1 Maldacena's conjecture

Maldacena's conjectured duality states that:

$$\mathcal{N}=4,\ D=4\ SU(N)\ SYM \equiv AdS_5 \times S^5$$

In this form of the correspondence the gauge theory on the boundary is a 4D super symmetric Yang Mills theory with four super symmetries and $SU(N)$ gauge symmetry. The theory is a conformal field theory. The gravitational theory is a string theory defined on a 5D anti-de Sitter spacetime times a 5-sphere.

The conjecture was made by looking at a D3 brane. This is an object which exists in theories of supergravity and string theory. Since string theory is 10 dimensional, a brane lives in a $9+1$ dimensional world, which means it has nine spatial dimensions and one time dimension. A D3-brane has infinite extension in three spatial dimensions and is a point object in the remaining six spatial dimensions [3]. The metric of a D3 brane is given by [15]:

$$ds^2 = \frac{-dt^2+dx_1^2+dx_2^2+dx_3^2}{\sqrt{1+L^4/r^4}} + \sqrt{1+L^4/r^4}\left(dr^2+r^2d\Omega_5^2\right) \tag{6.1}$$

In the near horizon limit $L >> r$ this metric reduces to:

$$ds^2 = \frac{r^2}{L^2}\left(-dt^2+dx_1^2+dx_2^2+dx_3^2\right)+\frac{L^2}{r^2}dr^2+L^2d\Omega_5^2 \tag{6.2}$$

Which is exactly the metric of AdS_5 plus a decoupled 5-sphere. This is the gravity side of the correspondence, now we will look at the other side. We will first look again at equation (3.6b), the metric of AdS_5 spacetime, which has a boundary at $z=0$. At the boundary, $dz=0$, the AdS_5 metric reduces to the 4D Minkowski metric except for an overall scaling factor, which means that the AdS spacetime at the boundary is conformally related to Minkowski spacetime. This makes it possible to define a CFT as the boundary theory since conformal field theories do not care about rescaling.

AdS_5 had one extra coordinate in comparison with 3+1D flat spacetime. This extra coordinate can be seen as the energy scale. Large z corresponds to small energy (IR) whereas small z means large energy (UV) [15]. This means that high energy physics on the boundary is described by bulk physics close to the boundary whereas low energy physics on the boundary is described by bulk physics closer to the horizon.

Figure 5 is a picture of AdS spacetime. It shows the conformal boundary at $r \to \infty$. It also shows that increasing r stretches spacetime.

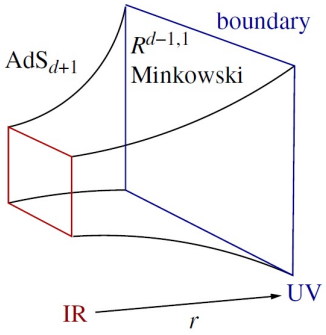

Figure 5: Anti-de Sitter spacetime [30]

Since the AdS/CFT correspondence is a duality, every excitation on the boundary must have a dual excitation in the bulk. For empty AdS the dual gauge theory is a theory at zero temperature. It is however more interesting to look at finite temperature gauge theories. But what happens to the bulk theory when we turn on the temperature on the boundary? It turns out that thermal excitations in the bulk are black holes. Since black holes have a naturally defined temperature this might not be that surprising. The empty $AdS_5 \times S^5$ metric changes to the Schwarzschild metric in AdS_5 plus the decoupled 5-sphere:

$$ds^2 = \frac{L^2}{z^2}\left(-f(z)dt^2 + dx_i^2 + \frac{1}{f(z)}dz^2\right) + L^2 d\Omega_5^2 \tag{6.3}$$

The Hawking temperature of a black hole is equal to the temperature of the gauge theory [24].

6.2 Relation between the parameters

In order to use the duality there has to be a relation between the gauge and gravity parameters. The bulk theory has the following parameters R, l_s and g_s where R is the AdS radius, l_s is the length of the string and g_s is the string coupling. The boundary theory has the parameters, g the coupling constant and N_c the number of colours. The parameters are related by the following equations [25]:

$$g^2 = 4\pi g_s \tag{6.4a}$$

$$g^2 N_c = R^4/l_s^4 \tag{6.4b}$$

$g^2 N_c$ is called the 't Hooft coupling. Since the gravitational side of the correspondence is a string theory it is in general difficult to use the correspondence. In the limit of large 't Hooft coupling and large N, string theory reduces to classical supergravity [20]. This can be seen from equation (6.4b), we see that $l_s \ll R$ in this limit. When the string length is smaller than the curvature radius the quantum corrections to classical gravity are small. Which means that string theory reduces to classical supergravity.

Using the correspondence it is possible to determine the properties of a strongly coupled CFT, by doing the calculations in the weakly coupled gravitational theory. As explained in section 2.2 it is usually extremely difficult to do calculations on strongly coupled systems. Weakly coupled systems however can be described using perturbation theory, which is easier. The AdS/CFT correspondence makes it thus a lot easier to determine the properties of the strongly coupled theory.

Observables in both theories can also be related, we already came across the fact that the Hawking temperature of a black hole is equal to the temperature of the SYM theory. The same holds for the entropy, the Bekenstein entropy of a black hole is equal to the entropy of a fluid in the SYM theory.

6.3 Remarks on the usability of the AdS/CFT correspondence

We had like to use the AdS/CFT correspondence to determine properties of the strongly coupled quark-gluon plasma. The problem is that QCD is not a conformal field theory, this makes it difficult to relate results from AdS calculations to properties of the QGP. Differences between QCD and the SYM plasma [15] are for example the fact that SYM is supersymmetric and has conformal invariance. This also means that SYM has an energy independent coupling constant. This in contrast to QCD which does not have supersymmetry and has a coupling constant which is energy dependent. Which results in asymptotic freedom. Another important difference between the two theories is the number of colours, N. The AdS/CFT correspondence is most useful in the strong coupling limit of the CFT, for which $N \to \infty$, but QCD has just $N = 3$. The differences become less dramatic if the temperature is non zero, because this 'breaks' the super symmetry [31].

It is hoped that despite these differences the correspondence offers some clues to the physics of the quark-gluon plasma. In chapter 8 we will see that it seems to give remarkably accurate predictions for some of the QGP properties, despite the mentioned differences. At the moment there is work being done to determine a gravitational theory whose dual theory is closer to QCD. But since QCD has less symmetries and no conformal invariance the gravitational dual is expected to be more difficult [32].

Besides applications to the QGP the correspondence is useful for other reasons:

First of all, since the AdS/CFT correspondence is a duality it can be used not only to determine properties of the strongly coupled gauge theory from calculations in a gravity theory but is can also be used the other way around. By doing calculations on the weakly coupled gauge theory it is possible to determine properties of the gravity theory which can not be determined otherwise. The duality itself is also useful in finding clues to the construction of a quantum field theory of gravitation, since the correspondence relates a quantum field theory with a gravitational theory [29].

7 Applying the AdS/CFT correspondence

We will now show how the AdS/CFT correspondence can be used to determine the η/s ratio of a deconfined plasma in the SYM theory. In order to do this the entropy and some other thermodynamic variables will be determined in the first section. The second part of this chapter will be concerned with determining the shear viscosity of a deconfined plasma. The first thing which has to be done is determining how shear viscosity causes a hydrodynamic wave to decay, this will be done in section 7.2. The simplest perturbations in the dual gravity theory are gravitational waves, in section 7.3 it will be determined how these waves decay in the presence of a black hole. Comparing these two calculations makes it possible to determine the viscosity and consequently the η/s ratio of a deconfined plasma in the SYM theory, this will be done in section 7.4. The remainder of this chapter will discuss the implications of the determined ratio.

7.1 Thermodynamic properties from AdS/CFT

The entropy of an AdS-Schwarzschild black hole can be determined as follows (from [25]). For a black hole in 4D the entropy is given by $S = \frac{c^3 A}{4G\hbar}$, were all the constants have been displayed. For a 10D black hole this law is still valid but we have to take the 10 dimensional gravitational constant. This is given by:

$$\sqrt{8\pi G_{10}} = 8\pi^{7/2} g_s l_s^4 \tag{7.1a}$$

This is given in string theory parameters, using equation (6.4a) and (6.4b) this formula can be written in terms of the CFT parameters.

$$G_{10} = \frac{1}{2N_c^2}\pi^4 R^8 \tag{7.1b}$$

Omitting again the constants except G_{10} we have:

$$S = \frac{A}{4G_{10}} \tag{7.2}$$

Now we will determine the area. This is determined from the metric of a black hole in $AdS_5 \times S^5$ given in equation (6.3). We look at the area at a constant time and at $z = z_0$ so the metric reduces to:

$$ds^2 = \frac{R^2}{z_0^2}(dx_1^2 + dx_2^2 + dx_3^2) + R^2\Omega_5^2 \tag{7.3}$$

The area of the horizon is given by:

$$A = \int \sqrt{g} dx_1 dx_2 dx_3 \cdot A_{S_5} \tag{7.4}$$

g is the determinant of the metric for the first 3 coordinates, $g = \frac{R^6}{z_0^6}$. A_{S_5} is the area of the 5-sphere, which is $A_{S_5} = \pi^3 R^5$. Plugging this into the previous equation we obtain:

$$A = \frac{R^8}{z_0^3}\pi^3 V_3 \tag{7.5}$$

V_3 is the volume of the x_1, x_2, x_3 dimension, these are extended into infinity so the volume is infinite. This will make the entropy infinite but it is possible to define a finite entropy density by dividing out this volume. Using the Hawking temperature of an AdS-Schwarzschild black hole $T = \frac{1}{\pi z_0}$ and equations (7.1b) and (7.2) the entropy density can be determined:

$$s = \frac{S}{V_3} = \frac{2R^8\pi^6 T^3 V_3 N_c^2}{4V_3\pi^4 R^8} = \frac{\pi^2}{2}T^3 N_c^2 \tag{7.6}$$

This value is remarkably similar to the entropy density of a gas of quarks and gluons in the $\mathcal{N} = 4$ SYM theory at zero coupling. Counting all degrees of freedom and using the fact that $N_c \gg 1$ this is given by [14]:

$$s_{free} = \frac{2\pi^2}{3}N_c^2 T^3 = \frac{4}{3}s \tag{7.7}$$

There is no contradiction in the fact that these two values for the entropy are not equal, since they are valid in different limits. s_{free} is valid for zero coupling whereas s is valid for a strongly coupled plasma.

Using equations (4.1b) and (4.1c) we can determine the pressure and energy density of the plasma [25]:

$$p = \int s dT = \frac{\pi^2 N_c^2 T^4}{8} \tag{7.8a}$$

$$\epsilon = Ts - p = \frac{3}{8}\pi^2 N_c^2 T^4 \tag{7.8b}$$

From these equations the equation of state can be read off, which gives $\epsilon = 3p$. This is exactly the equation of state of a conformal fluid.

The same calculations can also be done for just the AdS_5 spacetime using a Kaluza-Klein reduction on S^5, which relates G_5 to G_{10}. This will give exactly the same result.

7.2 Shear modes in a fluid from hydrodynamics

Every fluid is able to support waves. Due to viscosity these waves will dissipate. To determine how waves behave in a fluid we will add a perturbation to the fluid and then linearise $T^{\mu\nu}$ to first order in these perturbations. Solving the resulting Navier-Stokes equations will give the behaviour of a wave in the fluid. We start with repeating the energy-momentum tensor as defined in section 5.1:

$$T^{\mu\nu} = (\epsilon + p)u^\mu u^\nu + p g^{\mu\nu} - \sigma^{\mu\nu} \tag{7.9}$$

In the Landau frame $\sigma^{\mu\nu}$ is zero for all components except for the ij components which are:

$$\sigma_{ij} = \eta\left(\partial_i u_j + \partial_j u_i - \frac{2}{3}\delta_{ij}\partial_k u^k\right) + \zeta\delta_{ij}\partial_k u^k \tag{7.10}$$

We will look at a stationary state, for which $u^\mu = (1,0,0,0)$, with constant ϵ and p in flat space time. To this state a small perturbation in the velocity will be added: $\Delta u^\mu = (0, v_x(t,y), 0, v_z(t,y))$ with $v_x, v_z << 1$, the perturbation only depends on t and y. The perturbation will to first order give the following energy-momentum tensor:

$$T^{\mu\nu} = \begin{bmatrix} \epsilon & (\epsilon+p)v_x & 0 & (\epsilon+p)v_z \\ (\epsilon+p)v_x & p & -\eta\partial_y v_x & 0 \\ 0 & -\eta\partial_y v_x & p & -\eta\partial_y v_z \\ (\epsilon+p)v_z & 0 & -\eta\partial_y v_z & p \end{bmatrix} \tag{7.11}$$

Plugging this tensor into equation (5.2) gives two non-trivial equations:

$$\partial_t v_x = \frac{\eta}{\epsilon + p}\partial_y^2 v_x \tag{7.12a}$$

$$\partial_t v_z = \frac{\eta}{\epsilon + p}\partial_y^2 v_z \tag{7.12b}$$

Now the perturbations have to be specified, we will assume that the perturbations are plane waves of the form $v_x \propto \exp(-i\omega_1 t + ik_1 y)$ and $v_z \propto \exp(-i\omega_2 t + ik_2 y)$. Putting this into the equations gives us the dispersion relations:

$$\omega_j = -i\frac{\eta}{\epsilon + p}k_j^2 \equiv -i\mathcal{D}k_j^2; \quad j = 1,2 \tag{7.13}$$

Looking back at the wavelike perturbation we see that this perturbation will decay as:

$$v_{x,z} \propto e^{-\mathcal{D}k_j^2 t} \cdot e^{ik_j y}; \quad j = 1,2 \tag{7.14}$$

From the above derivation it can be concluded that in a viscous fluid wavelike perturbations will decay. How quickly these waves decay depends on the viscosity; the higher the viscosity the faster the waves dissipate. The perturbation used here will generate shear modes, using other perturbations can generate sound modes. Shear modes only depend on the shear viscosity whereas sound modes also depend on the bulk viscosity. This calculation can be generalized to perturbations in the metric, pressure and/or energy density (see for example [25] [23] and [33]). These all give the same dispersion relation for the shear modes.

7.3 Perturbations in a gravitational field

We will be looking at a perturbation in the AdS-Schwarzschild spacetime. In the presence of the black hole these waves will decay. In order to determine the diffusion constant of the gravitational theory several things have to be done. We will give a brief outline of the procedure here, but not do the complete derivation, this can be found in for example [25].

First a small perturbation is added to the exact Schwarzschild-AdS metric: $h^{\mu\nu}$, which has the following form $h^{\mu\nu} = A^{\mu\nu}e^{-i\omega t+ikx}b(z)$. $A^{\mu\nu}$ is a constant. Next the Einstein equations will be linearised. Before moving to the next step we will first show how to linearise the Einstein equations for perturbations around the Minkowski metric [12], this can be generalized to perturbations in an AdS-Schwarzschild background. The linearised Einstein equations are the weak field limit of the Einstein equations, they are only valid when the change to the spacetime due to matter and energy is small.

Linearising the Einstein equations

We will look at a perturbation in flat spacetime: $g_{\mu\nu} = \eta_{\mu\nu} + \epsilon h_{\mu\nu}$, with $\epsilon \ll 1$. $h_{\mu\nu}$ is a symmetric tensor which depends on all coordinates. We will assume that the metric is well-behaved, such that the partial derivatives commute. Since the metric always obeys $g^{\mu\nu}g_{\nu\rho} = \delta^\mu_\rho$ the inverse of this metric has to be $g^{\mu\nu} = \eta^{\mu\nu} - \epsilon h^{\mu\nu}$, such that $g^{\mu\nu}g_{\nu\rho}$ is equal to δ^μ_ρ up to first order in ϵ. The linearised Einstein equations can be determined by plugging this metric into the Einstein equation and keeping only the terms which are first order in ϵ. All indices run from 0 to 3.

First we will look how the perturbation changes the Christoffel symbols. Plugging the perturbed metric into equation (3.3a) we obtain:

$$\Gamma^i_{kl} = \frac{1}{2}\left(\eta^{im} - \epsilon h^{\mu\nu}\right)\epsilon\left(\frac{\partial h_{mk}}{\partial x^l} + \frac{\partial h_{ml}}{\partial x^k} - \frac{\partial h_{kl}}{\partial x^m}\right) \tag{7.15}$$

Since the Minkowski metric is just a constant the derivatives contain only $h_{\mu\nu}$. Keeping only the terms which are first order in ϵ we obtain:

$$\Gamma^i_{kl} = \frac{\epsilon}{2}\eta^{im}\left(\frac{\partial h_{mk}}{\partial x^l} + \frac{\partial h_{ml}}{\partial x^k} - \frac{\partial h_{kl}}{\partial x^m}\right) \tag{7.16}$$

Now this will be plugged into equation (3.3b) to determine the Riemann tensor. On first sight we can immediately neglect the last two terms, because the Christoffel symbols are first order in ϵ, these will be second order. The remaining two terms will give:

$$R^\alpha_{\mu\nu\rho} = \frac{\epsilon}{2}\eta^{\alpha m}\left[\partial_\nu\partial_\mu h_{m\rho} - \partial_\nu\partial_m h_{\mu\rho} - \partial_\rho\partial_\mu h_{m\nu} + \partial_\rho\partial_m h_{\mu\nu}\right] \tag{7.17}$$

Using this equation the Ricci tensor can be determined:

$$R_{\mu\nu} = \frac{\epsilon}{2}\left[\partial^m\partial_\mu h_{m\nu} - \partial^m\partial_m h_{\mu\nu} - \partial_\nu\partial_\mu h^m_m + \partial_\nu\partial^m h_{\mu m}\right] \tag{7.18a}$$

The curvature scalar is defined as $R = g^{\mu\nu}R_{\mu\nu}$ but since $R_{\mu\nu}$ is already first order in ϵ this can be approximated by $R = \eta^{\mu\nu}R_{\mu\nu}$, which result in the following curvature scalar

$$R = \frac{\epsilon}{2}\left[\partial^m\partial^\nu h_{m\nu} - \partial^m\partial_m h^\nu_\nu - \partial_\nu\partial^\nu h^m_m + \partial_\nu\partial^m h^\nu_m\right] \tag{7.18b}$$

Defining $\Box \equiv \partial_\mu\partial^\mu$, $h \equiv h^m_m$ and grouping terms this can be written in a nicer form:

$$R = \epsilon\left[\partial^\mu\partial^\nu h_{\mu\nu} - \Box h\right] \tag{7.18c}$$

Now these equations can be plugged into the Einstein equations, again $g_{\mu\nu} \approx n_{\mu\nu}$. This gives:

$$16\pi G T_{\mu\nu} = \epsilon\left[\partial^m\partial_\mu h_{m\nu} - \Box h_{\mu\nu} - \partial_\nu\partial_\mu h + \partial^m\partial_\nu h_{\mu m} - \partial^\alpha\partial^\beta h_{\alpha\beta}\eta_{\mu\nu} + \Box h n_{\mu\nu}\right] \tag{7.19}$$

The number of terms can be reduced by defining a new tensor:

$$H_{\mu\nu} = h_{\mu\nu} - \frac{1}{2}\eta_{\mu\nu}h \tag{7.20}$$

This tensor has the property: $H = -h$, with $H \equiv H^{\alpha}_{\alpha}$, just like $h_{\mu\nu}$ it is also symmetric. Plugging this into the Einstein equation and grouping the equal terms results in

$$16\pi G T_{\mu\nu} = \epsilon \left[\partial^m \partial_\mu H_{m\nu} + \partial^m \partial_\nu H_{\mu m} - \Box H_{\mu\nu} - \partial^\alpha \partial^\beta H_{\alpha\beta} \eta_{\mu\nu} \right] \tag{7.21}$$

This is the linearised Einstein equation, it is a second order differential equation. Just like QED and QCD, general relativity is also invariant under gauge transformations. More specifically, general relativity is invariant under coordinate transformations. In order to solve these equations we have to fix the gauge. The most commonly used gauge is the de Donder gauge (also called harmonic coordinate condition) which puts the following condition on the coordinates: $\partial^\mu H_{\mu\nu} = 0$. This gauge results in a very simple form of the linearised Einstein equations since all terms on the RHS, except for the third term, vanish. We end up with:

$$16\pi G T_{\mu\nu} = -\epsilon \Box H_{\mu\nu} \tag{7.22}$$

In the vacuum this solution simplifies even further to:

$$\Box H_{\mu\nu} = 0 \tag{7.23}$$

where ϵ has been omitted. The solution to this equation is just a plane wave:

$$H_{\mu\nu} \propto A_{\mu\nu} e^{-i\omega t + i\vec{k}\cdot\vec{x}} \text{ with } \omega^2 = |\vec{k}|^2 \tag{7.24}$$

$A_{\mu\nu}$ is again just a constant matrix. From the relation between ω and k it can be concluded that this plane wave travels with the speed of light. These waves are called gravitational waves.

The same procedure can be used to determine the linearized Einstein equations for a Schwarzschild-AdS background, but this will be more complicated since the Schwarzschild-AdS metric is not a constant like the Minkowski metric.

The next step is solving these linearised Einstein equations. We will now explain how linearized Einstein equations can be solved to obtain a dispersion relation.

Boundary conditions

The linearized Einstein equations are in general second order differential equations, the solution consists out of two linearly independent solutions. The complete solution will look like: $b(z) = c_1 b_1(z) + c_2 b_2(z)$. Solving this equation will however not give a unique solution for ω and k. In order to get a unique solution two boundary conditions have to be imposed:

At $z = 0$, the AdS boundary
Here the condition is imposed that the solution must be normalizable. If this condition is not imposed the amplitude keeps increasing which gives rise to infinite energies. This first condition will in general delete one of the two linearly independent solutions.

At $z = z_0$, the horizon
Here an in-falling condition is imposed, the waves at the horizon have to move towards the black hole centre. This is done to prevent waves from moving out of the black hole, which is unphysical.

Imposing both boundary conditions at the same time is only possible for specific values of ω and k. These boundary conditions will thus give us the dispersion relation. From this dispersion relation the diffusion constant can be determined. In [25] it is derived that shear modes decay with $\mathcal{D} = \frac{1}{4\pi T}$.

In appendix B we will show how these boundary conditions are imposed on the Klein-Gordon equation in an AdS-Schwarzschild background.

7.4 Viscosity over entropy density

We are now able to determine η/s from the results of the previous sections. But before doing the exact computation we will first give a hand waving argument of what we expect η/s to be. From the Bekenstein entropy we know that the entropy of a black hole is proportional to the area. The shear viscosity of a black hole is proportional to the absorption cross section of low energy gravitons [27]. Since cross sections are proportional to area we get the following result for η/s:

$$\frac{\eta}{s} \propto \frac{\sigma}{A} \propto \frac{A}{A} = 1 \tag{7.25}$$

This shows that we expect the ratio to be a constant.

Now the exact computation:
The entropy density of the Schwarzschild-AdS black hole is equivalent to the entropy density of the fluid, which is $s = \frac{\pi^2}{2} T^2 N_c^2$, as determined in section 7.2. The viscosity is found by comparing the decay rate of gravitational perturbations with the decay rate of waves in a fluid. Comparing these we obtain a formula for the viscosity:

$$\mathcal{D} = \frac{1}{4\pi T} = \frac{\eta}{\epsilon + p} \Rightarrow \eta = \frac{\epsilon + p}{4\pi T} \tag{7.26}$$

There are a couple of ways to determine η/s from this equation. The fastest one is to use equation (4.1c): $\epsilon + p = Ts$. This immediately gives $\eta/s = 1/4\pi$. The second way is to use the equations for energy density and pressure derived in section 7.1 to first determine the viscosity and then divide this by the entropy density. This again gives the same viscosity to entropy density ratio.

Concluding, using the AdS/CFT correspondence the viscosity to entropy density ratio can be determined. It is derived that:

$$\frac{\eta}{s} = \frac{1}{4\pi} \tag{7.27}$$

Viscosity bound

In [34] it is proposed that $\eta/s = 1/(4\pi)$ is a universal lower bound. The authors propose that every relativistic quantum field theory at non zero temperature and with no chemical potential has a viscosity to entropy density larger or equal to this bound. They furthermore propose that all relativistic quantum field theories with a gravity dual have $\eta/s = 1/(4\pi)$.

In figure 6 the viscosity to entropy density ratio as a function of the temperature for some well known fluids is compared to the viscosity bound. This figure clearly shows that η/s of the SYM fluid is a lot smaller than η/s of the other fluids. Even helium, which gets closest to this value, is still larger by a factor of about 10. This means that the SYM fluid is the most perfect fluid known, as already mentioned a perfect fluid has $\eta/s = 0$.

A second striking feature of this figure is that in the liquid phase the ratio goes down for increasing temperature whereas in the gas phase the ratio increases with increasing temperature. This is in accordance with that which was explained in section 5.2.

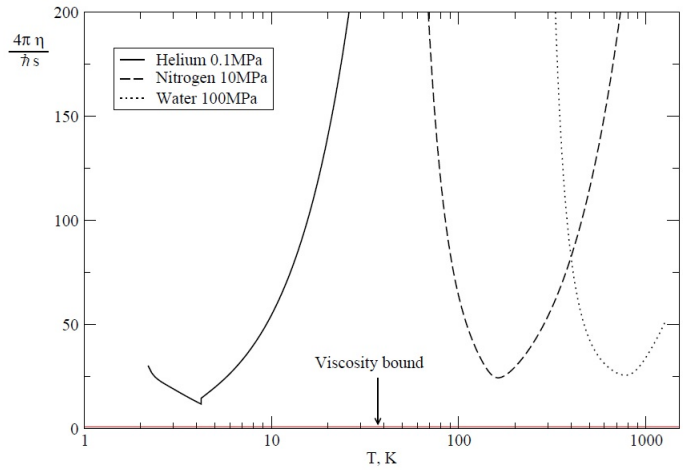

Figure 6: η/s for some substances, compared to the bound given by $\frac{4\pi\eta}{\hbar s} = 1$ [34]

8 Experiments

This chapter will first discuss more extensively what the QGP is and how it can be created in experiments. Thereafter some details of the RHIC experiment will be given. Then the experimental results from RHIC will be discussed, we end this section with some concluding remarks.

8.1 The Quark-Gluon Plasma

The quark-gluon plasma is a state of matter which is created at large energy densities, at these high energy densities the matter undergoes a transition from the confined state (hadrons) to the deconfined state (plasma). A minimal definition of the QGP is given in [35] as: *"A locally thermally equilibrated state of matter in which quarks and gluons are deconfined from hadrons, so that colour degrees of freedom become manifest over nuclear rather than nucleonic volumes"*. We know that in the confined state colour is only present inside the nucleon (in the form of quarks and gluons) since all nucleons, or more general hadrons, are colour neutral. Deconfinement means that colour is present on larger scales than the nucleon size.

Simple models produce a transition energy around 150MeV [1]. The position can be determined more precisely using lattice QCD, which can determine ϵ/T^4 as a function of the temperature. This is shown in figure 7. The three lines represent the different quark configurations (3=three light quarks; 2+1=two light quarks and one heavier quark; 2=two light quarks) for which the lattice calculations are done. The figure shows a dramatic, fast increase in ϵ/T^4 around a certain critical temperature (T_c), similar to for example the liquid to gas phase-transition in water. This increase indicates that the number of degrees of freedom increases, which is a sign that there is a transition from a confined to deconfined state. The transition temperature is calculated to be around 170MeV, which is equivalent to an energy density of $1GeV/fm^3$. For comparison; a single proton has an energy density of $\sim 350MeV/fm^3$ whereas a gold nucleus has an energy density of $\sim 100MeV/fm^3$ *. The energy density of the QGP is thus much larger than the typical nuclear energy densities, which shows that hadrons overlap and are thus no longer distinguishable.

In the figure the Stefan-Boltzmann limit is indicated by the arrows on the right hand side. This limit is valid for a gas of non-interacting particles. Since the saturation limit is well below this value we can conclude that lattice QCD predicts that even above the transition temperature the plasma still has some interaction.

*The energy densities of the proton and gold nucleus are determined by dividing the mass of the nucleus by its volume. The volume is calculated from the charge radius of the nucleus.

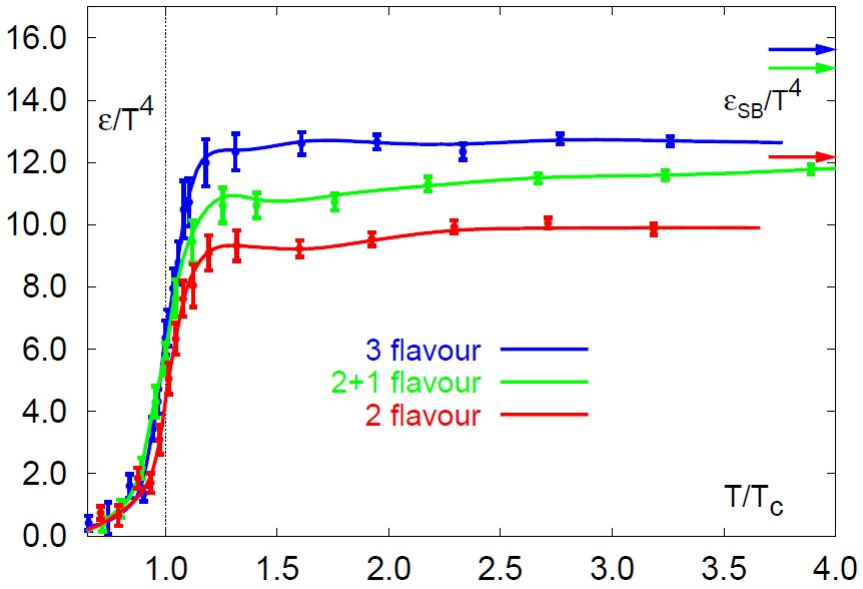

Figure 7: Lattice QCD results, the figure shows a phase transition at a critical temperature of about $T_c = 170MeV$ [35]

8.2 How to create a quark-gluon plasma in experiments?

QGPs are created by colliding nuclei with relativistic energies. The high amount of energy available in the collisions will ensure the creation of a region with a high enough energy density. Nuclei with a large number of nucleons are used, because this will result in a lot of particles (quarks and gluons) with $l \ll L$. This makes it possible to create a state for which statistical (hydro- and thermodynamic) properties can be defined [36].

After the initial collision and the creation of the QGP, the QGP will start to expand due to the internal pressure. This expansion will result in a decreasing temperature which will in turn increase the interaction strength. Quarks and anti-quarks are now able to recombine into hadrons; the quark-gluon plasma starts to evaporate. This is called hadronization. The lifetime of the QGP created at RHIC is about $4 \times 10^{-23}s$ [6]. Figure 8 shows very schematically the different phases of QCD, μ is the baryon chemical potential. Increasing the baryon chemical potential is basically equivalent to compressing hadrons, which can also result in a deconfined state. We see that above a certain temperature a QGP will always be created, independent of the value of μ.

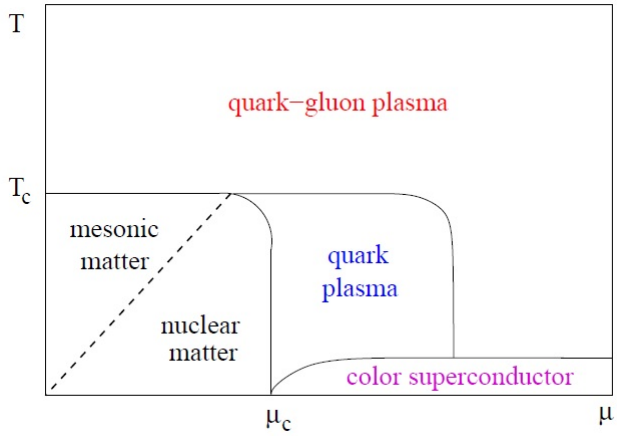

Figure 8: Phase diagram of QCD states of matter [1]

The QGP can only be investigated indirectly by measuring the created hadrons and leptons and their properties. Direct measurement of a deconfined quark or gluon is not possible due to colour confinement. This makes it more difficult to prove that a QGP is created and to determine its properties.

The two main facilities where they do these kinds of experiments are the Relativistic Heavy Ion Collider (RHIC) at the Brookhaven National Laboratory (BNL) and the LHC at CERN. The main goal of the experiments is to detect signatures of the creation of the QGP and measure its properties. The most important difference between these two experiments is the energy at which they collide ions. Whereas RHIC collides nuclei with a centre of mass energy of 200GeV per nucleon pair, the LHC is able to reach centre of mass energies of 5.5TeV per nucleon pair. Since the RHIC experiment was the first to show that it is possible to create a new state of matter by colliding nuclei this chapter will mostly focus on the RHIC experiment and its results.

The RHIC facility and its detectors

The RHIC facility is schematically drawn in figure 9. Information on the RHIC experiment and the detectors is taken from [37].

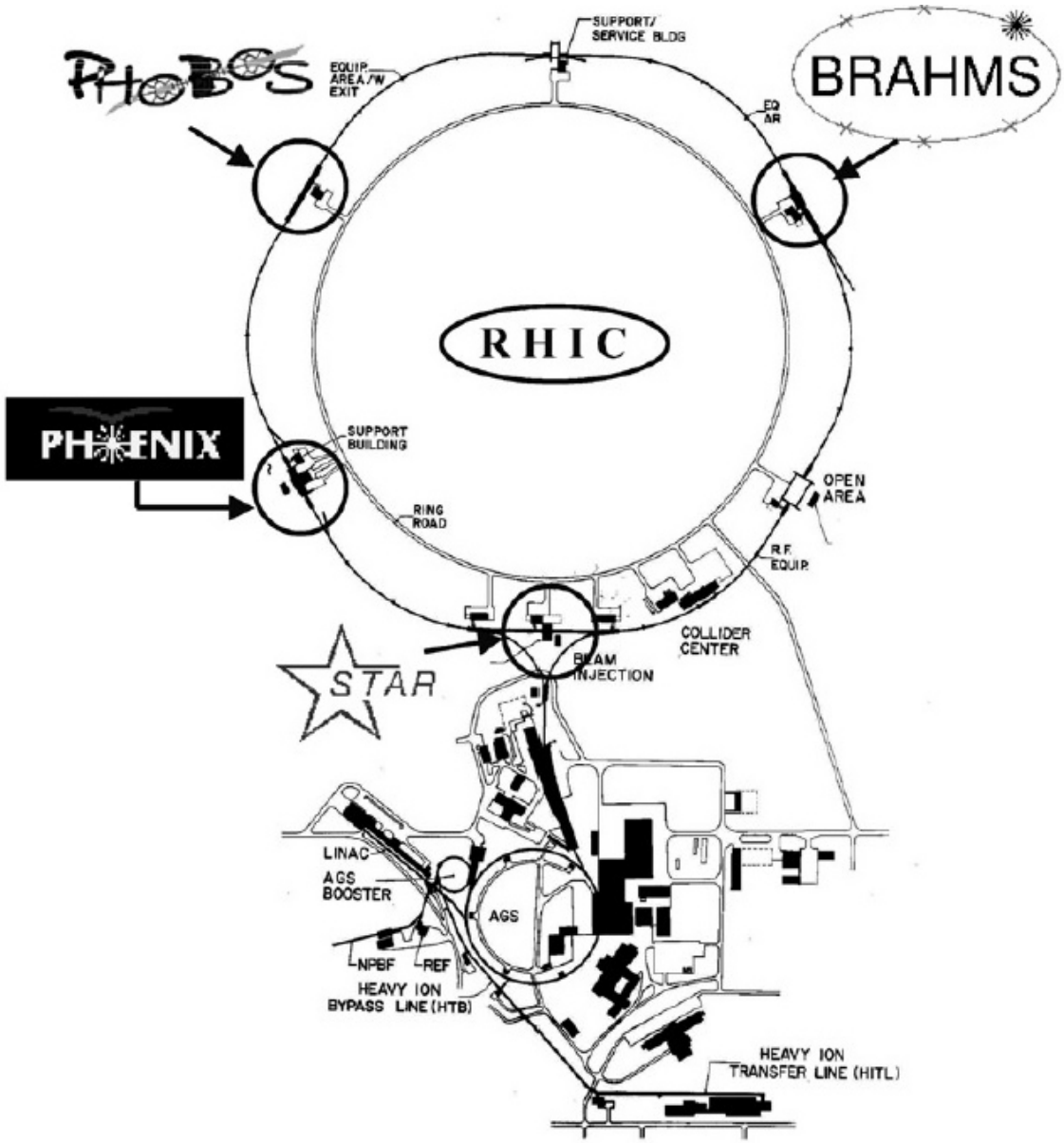

Figure 9: Schematic overview of RHIC, the collider and its detectors [37]

Nuclei will first be accelerated and completely ionized in smaller facilities (bottom of picture). The beams will then be injected into the main collider, which accelerates the particles even further. The collider consists out of two rings, in one of the rings a beam is moving clockwise in the other counter-clockwise. The counter-rotating beams will be collided at the intersection points, around which the detectors are build. Both rings have independent sources which makes it possible to collide different ions (for example p+Au). Using counter rotating beams instead of fixed target collisions results in an extreme increase in the centre of mass energy, which makes it more likely that the required energy density is reached.

The four detectors which measure the collisions are STAR, PHENIX, PHOBOS and BRAHMS. They are all designed for specific measurements but they are also able to cross check each others measurements. The detectors measure not only the particles which are created during the hadronization phase, but also photons and leptons which are created earlier. The detectors identify the hadrons and measure their paths, they also measure the momentum and energy of these particles.

So far RHIC has done several collisions, for example, Au+Au and d+Au collisions. RHIC does experiments at different energies to look for the exact transition moment. This is done to study what kind of transition there is between the deconfined and confined state (e.g. first order phase transition, continuous transition). The experiment just (2015) started a new run which will look at p+Au collisions. The collisions of large ions with a proton or deuteron are mainly done to establish a baseline. Since we do not expect a QGP to form here all effects which are present in these collisions as well as the Au+Au collisions have other origins than interactions with the QGP.

The LHC looks mainly at Pb+Pb and p+p collisions. These experiments are done to determine what happens to the strong interaction and the QGP at even higher energies than the energies reached at RHIC.

8.3 Some basics of heavy ion collisions

Centrality

Most collisions between nuclei are not head-on but have some non zero impact parameter b, this is schematically drawn in figure 10. Non-central collisions will result in an almond shaped reaction region. The particles outside this region are called the spectator particles and do not take part in the collision. How large the spatial anisotropy is can be described by the eccentricity (ϵ), which is defined as [38]:

$$\epsilon = \frac{\langle y^2 - x^2 \rangle}{\langle y^2 + x^2 \rangle} \tag{8.1}$$

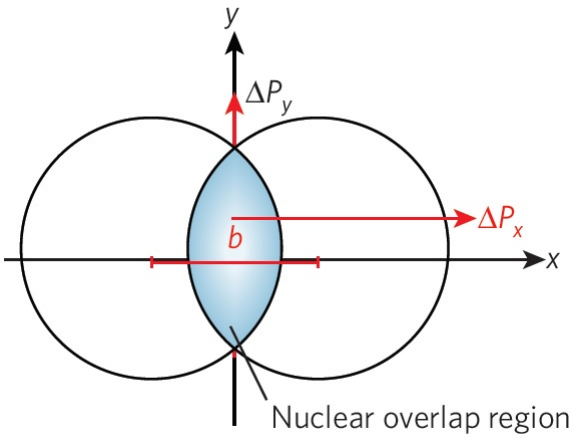

Figure 10: A non central collision between two nuclei, as seen from the collision plane [39]

Flow harmonics

Due to spatial anisotropy there will be an anisotropy in the number of emitted particles in the plane transverse to the beam direction. This anisotropy can be decomposed in Fourier components as:

$$\frac{dN}{d\phi} \propto 1 + 2\sum_{n=1}^{\infty} v_n \cos[n(\phi - \Phi_n)] \tag{8.2}$$

v_n are called the flow harmonics. v_2 is the elliptic flow parameter which will be discussed next.

Elliptic flow

Elliptic flow if a flow which has an asymmetry in the collision plane transverse to the beam. If the collision is non-central and the interaction strength non zero elliptic flow is created. The non-central collision result in a spatial anisotropy. Interactions will consequently result in a momentum anisotropy. This happens because particles moving along the long axis (y direction) will have a higher probability to scatter than particles moving along the short axis (x direction). This means that more particles will be emitted in the x direction [40]. In total the momentum of the emitted particles will have $p_x > p_y$.

The momentum anisotropy as a result of the spatial anisotropy depends strongly on the interaction strength. If there is no interaction at all, the spatial anisotropy will not result in a momentum anisotropy because there will be no scatterings. A large elliptic flow thus indicates that the system is strongly interacting and can be described by hydrodynamics.

The momentum anisotropy due to spatial anisotropy can also be explained using hydrodynamics; the shorter axis has a higher pressure which will result in a faster expansion. This will thus result in a momentum anisotropy, more higher momentum particles are emitted along the short axis.

The elliptic flow depends strongly on the η/s ratio of a system, hydrodynamic simulations show that a small increase of η/s already decreases the elliptic flow by a large amount, see for example figure 12.

During the expansion of the QGP the initial spatial anisotropy and thus the creation of elliptic flow disappears. This means that most of the elliptic flow is formed in the early phases after the collision, where there is still a 'pure' QGP and not much hadronization. This makes elliptic flow especially useful in determining the properties of the QGP [41].

To compare simulations to experiments the elliptic flow parameter is integrated over either the impact parameter or the transverse momentum. These are called the minimum bias elliptic flow and the integrated elliptic flow parameter, respectively. The transverse momentum p_T is defined as $\sqrt{p_x^2 + p_y^2}$.

Jets

The collision creates a lot of coloured particles, like gluons and quarks. Since these particles can not remain as individual coloured particles, due to confinement, they will create lots extra $q\bar{q}$-pairs when they fly off. This will combine, which results in lots of colour neutral hadrons. These particles will all move in the same general direction and form a jet.

8.4 Experimental results from RHIC

First we will briefly explain how the experimental results show that a QGP has formed. In the second part it will be shown how the η/s ratio can be extracted from measurements.

8.4.1 Does a QGP form?

In order to show that a QGP forms we first have to show that the energy density is high enough, otherwise it is not even possible to create a QGP. In [35] the energy density is estimated from experimental data of Au+Au collisions at RHIC. This is done by looking at the energy loss of the colliding nuclei and the number of produced particles. These calculations indicate an energy density of at least $5GeV/fm^3$. Which is well above the critical density of $1GeV/fm^3$. The main condition to create a QGP is thus met.

The defining property of the QGP is deconfinement of colour. If measurements show that colour is deconfined over a region larger than the size of a nucleon, we have strong indication that the QGP is formed. The main indication of colour deconfinement is the so called jet-quenching. Jet-quenching means that particles/jets with high transverse momentum are suppressed, in comparison with particle momenta of p+p collisions.

Jet quenching can be caused by two separate effects. The first explanation is that particles interact strongly with the deconfined QGP, these scatterings results in energy loss and thus suppression of the high momentum particles. The energy loss depends on the distance travelled trough the medium. The second explanation is that jet-quenching is caused by an initial state effect due the fact that we are colliding nuclei instead of single nucleons (called gluon saturation). This will result in the creation of a smaller number of jets. Both effects are capable to produce the measure jet-quenching in Au+Au collisions.

How can we distinguish between energy loss on the one hand and initial state effects on the other hand? This can be done by looking at d+Au collisions. Since we are still colliding a nucleus the initial effects would be still present in some form. The energy loss due to the interaction with the QGP will disappear however, since we do not expect a QGP to form in d+Au. Even if a QGP does form it will be small, since less nucleons are available in the collision, which would still cause the energy loss to disappear.

In figure 11 Au+Au and d+Au collisions are compared to p+p collisions using the ratio R. The ratio is a measure of the number of particle created. It is clearly visible that for high p_T the number of particle drastically decreases in Au+Au collisions, this is the jet quenching. However we do not see this effect in d+Au collisions. This shows that jet-quenching can not be an initial state effect but must be due to the interactions with the quark-gluon plasma.

The observed jet-quenching, absent in p+Au collisions but observed in Au+Au collisions, thus shows that a QGP is created in Au+Au collisions [42]. Nowadays there is general agreement that QGPs are formed in heavy ion collisions at RHIC and the LHC.

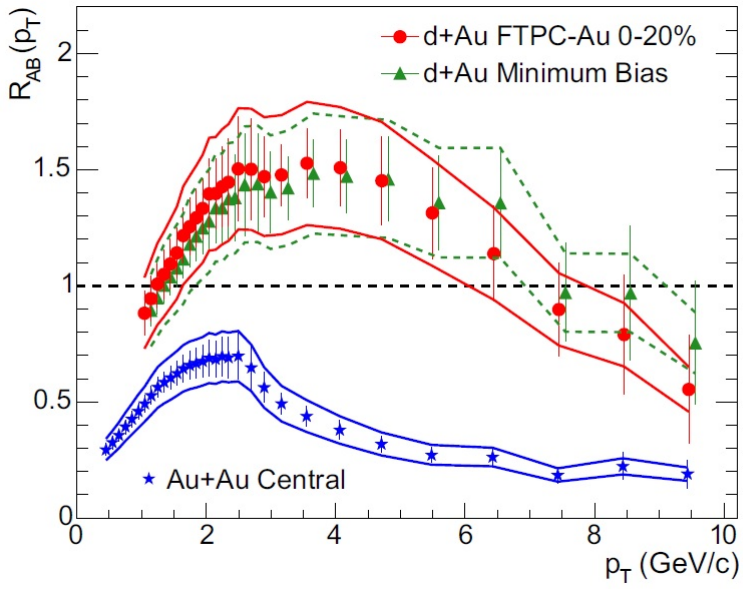

Figure 11: Jet quenching in Au+Au collisions, jet quenching is absent in d+Au collisions [42]

8.4.2 Extracting η/s

η/s can not be determined directly from measurements, the only way to determine it from experiment is by comparing experimentally measurable parameters with models of the plasma. By plugging in different η/s values into these models the best fit to the data can be determined. This gives an indirect determination of η/s.

The difficult part is making a suitable model. The first problem is determining the initial state, which is not known exactly. This uncertainty in the initial states results in some uncertainty in the calculations of the model. A second problem is the hadronization, at this point hydrodynamics is not valid any more, the model should take this into account. A model for hadronization is needed to determine the final hadron distribution, which can then be compared with experimental results.

Since the initial conditions are not known to high precision, we must look at parameters which do not depend much on the initial conditions chosen in order to get a precise extraction of η/s. The parameters chosen should however be sensitive to η/s to get a more precisely determined value. The elliptic flow satisfies both conditions which makes it useful as parameter to determine η/s [35].

The initial conditions

The energy density in the beam direction is assumed to be boost invariant. This makes the problem 2+1 dimensional instead of 3+1 dimensional. This still leaves the energy density in the reaction plane undetermined. The energy density is usually determined by either a Glauber type model or a Color-Glass-Condensate type model (CGC or KLN). Whereas the Glauber model determines the initial energy density from the nucleon distribution, the CGC model determines the initial energy density from the gluon distribution. The two models we will discuss use both methods to determine the initial energy density, which makes it possible to compare them.

The models

- Model 1 (2009) [43]:
  This model uses relativistic viscous hydrodynamics which also includes second order dissipative effects (hydro with only first order derivatives has some problems with causality). The model assumes that the bulk viscosity can be neglected. Other details on the initial state assumptions can be found in the cited paper. The hadronization is taken into account using a instantaneous freeze-out model described by the Cooper-Frye equation. The Cooper-Frye equation determines the number of particles formed per particle specie in the hadronization phase of the plasma. The number of created particles depends on the mass of each specie. The equation is thus able to determine the final hadron distributions created from the fluid after hadronization. The freeze-out model assumes that the hadrons, once created, do not interact after the sudden hadronization.

- Model 2 (2011) [44]:
  This is a hybrid model. It first uses viscous hydrodynamics to describe the QGP, than it switches to a hadron scattering model to describe the hadronization and the interaction between hadrons. The second part is described on microscopic scale. This hadron cascade model assumes gradual instead of sudden freeze-out. The model also assumes the bulk viscosity to be zero. The equation of state is based on lattice QCD calculations.

Whereas the first model assumes instantaneous freeze-out the second model assumes a gradual freeze-out during which the hadrons are still able to interact. Hadronization reduces the elliptic flow [45] and thus changes the average η/s. Taking into account these gradual hadronization effects gives a more precise value for η/s of the quark-gluon plasma.

Results

Figure 12 and figure 13 show the results of model 1 and 2, respectively. Figure 12 shows the elliptic flow as a function of the particle number and as a function of the transverse momentum. The figures on the left show the integrated elliptic flow whereas the figures on the right show the minimum bias elliptic flow. Figure 13 shows the average elliptic flow divided by the eccentricity as a function of the multiplicity per area. The results of the model for different η/s are compared to experimental results to find the best fit.

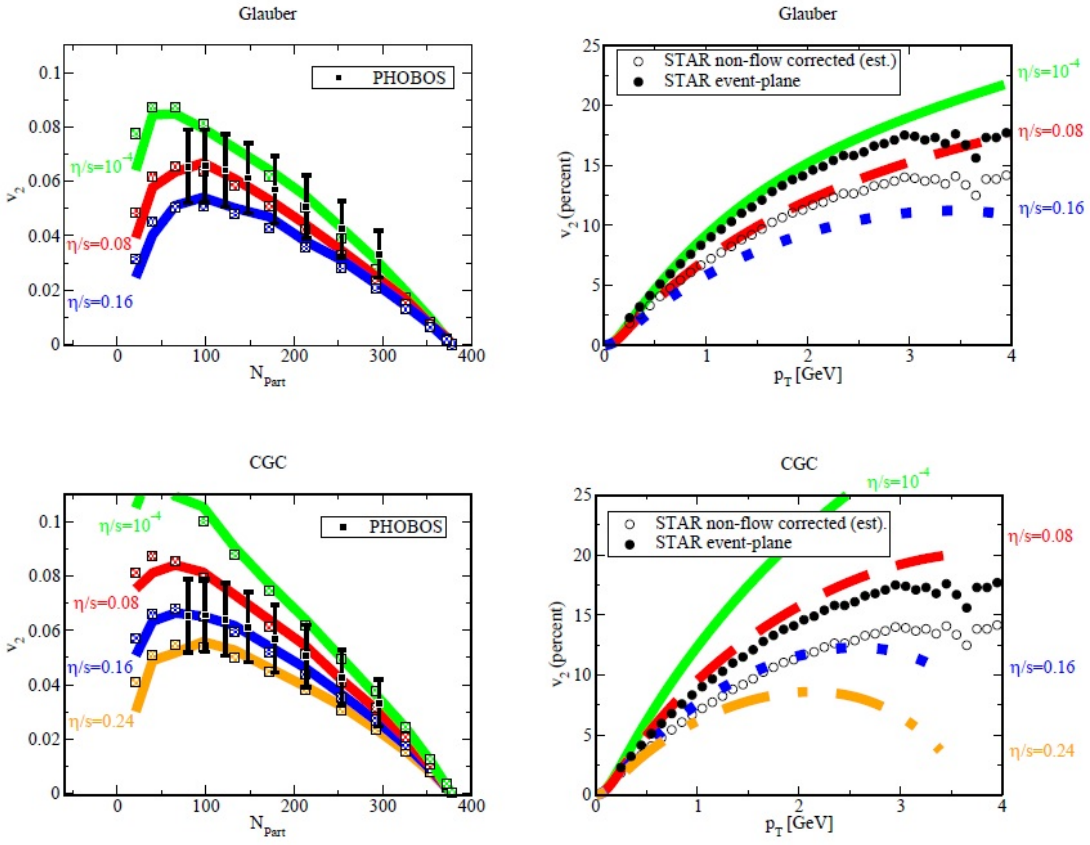

Figure 12: Model 1: determining $\frac{\eta}{s}$ of the QGP, using a second order hydro model [43]

3

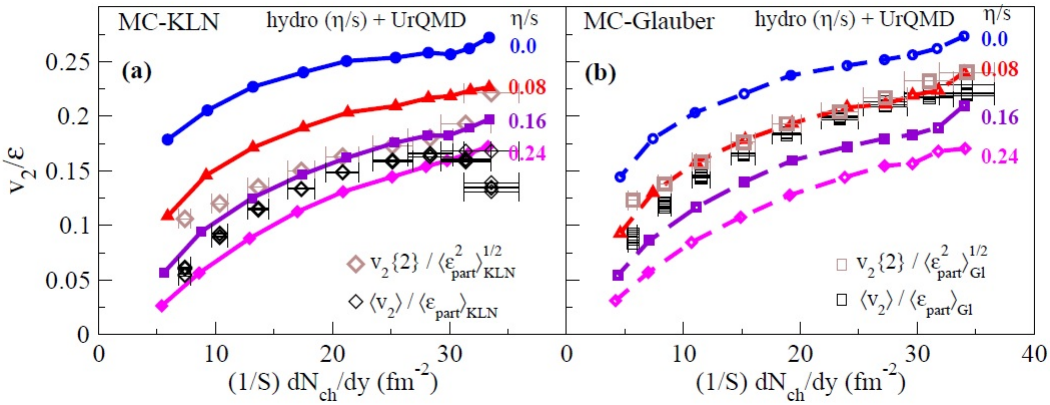

Figure 13: Model 2: determine $\frac{\eta}{s}$ of the QGP, using a hybrid model [44]

The models put the following bounds on η/s of the QGP:

- Model 1 can with high certainty put an upper bound on the ratio: $\eta/s < 0.5 \sim 6\frac{1}{4\pi}$.
- Model 2 is able to determine a smaller upper bound for η/s. The authors state the following upper and lower bound: $0.08 < \eta/s < 0.2$ or in terms of $\frac{1}{4\pi}$: $\frac{1}{4\pi} < \eta/s < 2.5\frac{1}{4\pi}$. This is the viscosity of the plasma for temperatures between $1 - 2 \times T_c$.

8.5 Concluding remarks

The models show that the hydrodynamics breaks down at $p_T > 2GeV$. This is to be expected since the higher momentum particles will scatter less often and will thus not be in thermal equilibrium with the surroundings [35].

The models agree that η/s is extremely small. The most recent model (model 2) gives an upper bound which is only a factor of 2.5 above the value predicted by the AdS/CFT correspondence. This means that the QGP behaves as an almost perfect fluid. The small ratio also shows that the interaction must still be relatively large. The QGP is thus not a weakly interacting system, as physicist first expected from asymptotic freedom.

Improving the bounds

From the models it can be seen that the Glauber model gives smaller values for the ratio than the CGC model. The determined ratios differ by a factor of about two. The different initial conditions (Glauber/ CGC) cause a large uncertainty in the determination of η/s. Constructing more accurate models for the initial conditions will decreases the uncertainty bounds on η/s.

In most models η/s is taken to be constant, independent of temperature. This behaviour does not fit with what we are used to for most fluids (see figure 6) which have viscosities which are usually strongly dependent on temperature. A model which incorporates a temperature dependent η/s would improve the agreement with experimental results.

There are still a couple of effects which these models neglect, for example the bulk viscosity. Taking these effects into account will also decrease the uncertainties in the determined ratio.

Hydrodynamics

Apart from describing the $v_2 - p_T$ curves reasonably well hydrodynamics is also able to predict the measured mass dependence of the $v_2 - p_t$-curve [35]. This is another indication that the quark-gluon plasma can be described accurately by hydrodynamics. From hydrodynamics we know that lighter particles should have larger v_2, an explanation of this phenomenon can be found in [46]. Figure 14 shows good agreement between hydrodynamic predictions and the experimental data, up to $1GeV/c$. It shows the expected mass ordering, the particle ordered from heavy to light are: Λ - p - K - π. Which is exactly the order which can be read of from the figure. This also shows that all the particles are emitted from the same expanding thermal source, close to kinetic equilibrium [40].

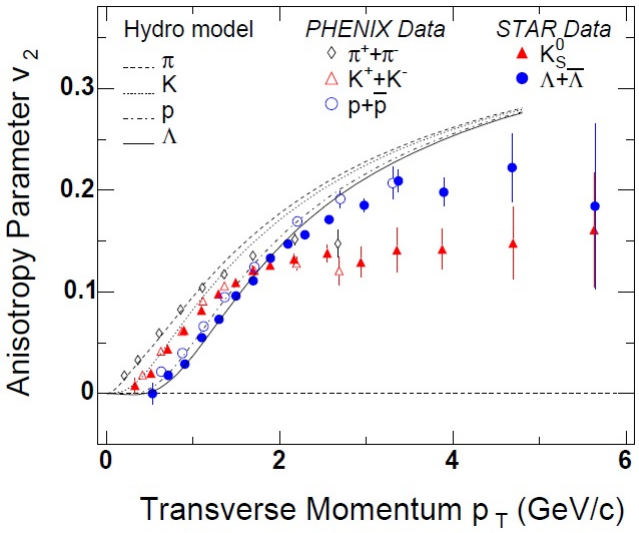

Figure 14: Mass dependence of the elliptic flow parameter, experimental data compared with hydrodynamic predictions [10]

9 Conclusion and Discussion

In this thesis we have been looking at the AdS/CFT correspondence and its application to the quark-gluon plasma. The AdS/CFT correspondence relates a strongly coupled gauge theory to a weakly coupled gravity theory. This makes it possible to determine dynamical properties of a strongly coupled system, which can not be determined using other methods. The QGP is a state of matter at extremely high energy densities, where the quarks and gluons are deconfined.

Using the correspondence we have determined the viscosity to entropy density ratio of a supersymmetric Yang Mills plasma. Briefly speaking the viscosity to entropy density ratio was determined by looking at the dissipation of shear waves in a fluid. This is compared to the dissipation of (shear) perturbations in the vicinity of a black hole to determine η/s. We have shown that η/s is equal to $1/(4\pi)$. At first sight it is not clear how this can be applied to the QGP since QCD is not a supersymmetric theory.

We compared this value to experimental results on the QGP. Historically the most interesting result from these experiments is the fact that η/s is quite small. Experiments show that η/s is at most $2.5 \times 1/(4\pi)$. This showed that the QGP is still relatively strongly coupled, contrary to previous believes that it is weakly coupled due to asymptotic freedom. The QGP η/s is remarkably close to the predicted value from the AdS/CFT correspondence for a supersymmetric plasma. The small η/s makes the QGP the most perfect fluid observed in nature.

It is interesting that such a small system (couple of thousand particles) can be described by hydrodynamics, this is only possible due to the almost completely perfect behaviour, small η/s, of the QGP. Another reason why such a small amount of particles can be described by hydrodynamics is the fact that quarks and gluons are almost point-like. This means that the systems size is not limited by the size of atoms, as is the case with water, for example [47].

Future goals

Unfortunately we are not able to predict η/s of the quark-gluon plasma from first principles. The method used nowadays is only indirect since it determines the viscosity to entropy density ratio by comparing hydrodynamic models to experimental results. Making a prediction of η/s from first principles can be achieved by two different roads. The first is to get a better understanding of lattice QCD to make it function to determine not only static properties but also dynamic properties of the QGP. A second road would be to determine the gravity dual of a gauge theory which is more like QCD.

Besides this, physicists are also working on getting a more accurate η/s ratio from experiments. This is done by doing more precise measurements and making more accurate models.

A Derivation of non-relativistic Navier-Stokes equation

This derivation is based on the book 'Fluid mechanics' by P. Kundu et al. [22]. The formula which imposes conservation of mass is:

$$\frac{d}{dt}\int_V \rho dV + \int_A \rho \vec{u}\cdot\vec{n}dA = 0 \tag{A.1a}$$

The velocity is the velocity of the flow with respect to the volume. This basically states that the flow into and out of the volume through a certain surface (2^{nd} term) must be accompanied by a change in the mass (1^{st} term). The formula which imposes momentum conservation is:

$$\frac{d}{dt}\int_V \rho\vec{u}dV + \int_A \rho\vec{u}(\vec{u}\cdot\vec{n})dA = \int_V \rho\vec{g}dV + \int_A \vec{f}dA \tag{A.1b}$$

The first term on the LHS is the change in momentum, the second term states how much momentum flows into volume when the volume or surroundings are moving. The first term on the RHS is the force acting on the volume (for example gravity) the last term is the force acting on the area surrounding the volume. Next we will use Gauss' theorem to make all integrals over volume instead of area. The integral can than be omitted. This gives for eq. (A.1a) and equation (A.1b):

$$\frac{\partial\rho}{\partial t} + \vec{\nabla}\cdot(\rho\vec{u}) = 0 \tag{A.2a}$$

and:

$$\frac{\partial}{\partial t}(\rho u_j) + \frac{\partial}{\partial x_i}(\rho u_i u_j) = \rho g_j + \frac{\partial}{\partial x_i}(\tau_{ij}) \tag{A.2b}$$

The stress tensor for a 3D flow is defined as follows for a Newtonian fluid

$$\tau_{ij} = -p\delta_{ij} + 2\eta(S_{ij} - \frac{1}{3}S_{mm}\delta_{ij}) + \mu_\nu S_{mm}\delta_{ij} \tag{A.3a}$$

$$\mu_\nu = \zeta + \frac{2}{3}\eta \tag{A.3b}$$

$$S_{ij} = \frac{1}{2}\left(\frac{\partial u_i}{\partial x_j} + \frac{\partial u_j}{\partial x_i}\right) \tag{A.3c}$$

η is the shear viscosity and ζ is the bulk viscosity. The bulk viscosity is related to how the fluid reacts when it is compressed (for example sound waves). Now we assume that the fluid is incompressible, this means that $\frac{\partial u_m}{\partial x_m} = 0$, so $S_{mm} = 0$. We also assume a constant density and constant viscosities, which makes it possible to take them out of the derivatives.

Combining these equations we obtain:

$$\rho\left[\frac{\partial\vec{u}}{\partial t} + \left(\vec{u}\cdot\vec{\nabla}\right)\vec{u}\right] = \rho\vec{g} - \vec{\nabla}p + \eta\nabla^2\vec{u} \tag{A.4}$$

B Imposing the boundary conditions

In this appendix we will show how the boundary conditions as explained in chapter 7.3 can be imposed on a toy model. The toy model which will be used is the Klein-Gordon equation in AdS spacetime. The Klein-Gordon equation is a relativistic form of the Schrödinger equation. The Klein-Gordon equation for a massless field is usually given as:

$$\Box\phi = 0 \tag{B.1a}$$

$$\Box = \partial_\mu \partial^\mu = -\partial_t^2 + \nabla^2 \tag{B.1b}$$

This equation is valid for flat spacetime. For a curved spacetime the Klein-Gordon equation changes to:

$$\frac{1}{\sqrt{-g}}\partial_\mu\left(\sqrt{-g}g^{\mu\nu}\partial_\nu\phi\right) = 0 \tag{B.2a}$$

g is defined as

$$g = \det g_{\mu\nu} \tag{B.2b}$$

and $g^{\mu\nu}$ is defined as:

$$g^{\mu\nu}g_{\nu\rho} = \delta^\mu_\rho \tag{B.2c}$$

At the AdS boundary

We will first look at the boundary condition for the AdS boundary. Since we will be looking at the boundary far away from a black hole it is possible to just use the metric for the empty AdS_5, which is given by:

$$g_{\mu\nu} = \frac{1}{z^2}\,\mathrm{diag}(-1,+1,+1,+1,+1) \tag{B.3}$$

with $L = 1$. For this metric the Klein-Gordon equation can be written as

$$z^5\partial_\mu\left(z^5 g^{\mu\nu}\partial_\nu\phi\right) = 0 \tag{B.4}$$

From equation B.2c we have $g^{\mu\nu} = z^2\,\mathrm{diag}(-1,+1,+1,+1,+1)$. Now we will define ϕ as:

$$\phi = e^{-i\omega t + i\vec{k}\cdot\vec{x}}b(z) \tag{B.5}$$

Plugging this into the Klein-Gordon equation, taken the derivatives and omitting the exponential term we get:

$$\left(\omega^2 - \vec{k}^2\right)z^2 b(z) + z^5\partial_z\left(z^{-3}\partial_z b(z)\right) = 0 \tag{B.6}$$

This is a second order differential equation (thus similar to what we expect to get from the linearisation of the Einstein equations). The exact solutions of this equation are two Bessel functions. Bessel functions can be expanded around $z = 0$ as: $b(z) = z^a(1 + c_1 z + \cdots)$. We are interested in the boundary so we will look at $z \to 0$. In this limit $b(z)$ can be approximated by $b(z) \approx z^a$. Plugging this into equation (B.6) and taken the remaining derivatives gives:

$$\left(\omega^2 - |\vec{k}|^2\right)z^{a+2} + a(a-4)z^a = 0 \tag{B.7}$$

But for small z the first term will always be smaller than the second term, this means that the second term has to be zero, which implies that $a = 0, 4$. We thus get two linear independent solutions for $b(z)$. The complete solution for ϕ is:

$$\phi = e^{-i\omega t + i\vec{k}\cdot\vec{x}}(b_1 z^0 + b_2 z^4) \tag{B.8}$$

Now we are able to impose the first boundary condition. Which states that the solution must be normalizable at the AdS boundary. Looking at the two terms we see that the first term is just a constant whereas the second term still depends in z. Close to the boundary this last term will vanish whereas the first term will stay a constant. This first term will have to be put to zero to make sure the energy will not become infinite. The solution now is

$$\phi = e^{-i\omega t + i\vec{k}\cdot\vec{x}}b_2 z^4 \tag{B.9}$$

Thus we see that imposing the first boundary condition on the solution of the Klein-Gordon equation results in the disappearance of one of the two linearly independent solutions.

At the horizon

Since we are now looking close to the horizon we will need to use the AdS-Schwarzschild black hole metric which is given by:

$$ds^2 = \frac{1}{z^2}\left(-f(z)dt^2 + dx_i^2 + \frac{1}{f(z)}dz^2\right); \quad f(z) = 1 - \frac{z^4}{z_0^4} \tag{B.10}$$

Again $L = 1$. Since this metric has a coordinate singularity at the horizon, the coordinates first have be to transformed in such a way that the singularity disappears. This can be done with the transformation: $dz^2 = f(z)^2 dz^{\star 2}$. Which changes the metric to:

$$ds^2 = \frac{f(z)}{z^2}\left(dt^2 + dz^{\star 2}\right) + \frac{1}{z^2}dx_i^2 \tag{B.11}$$

This metric does not have a singularity at the horizon. These coordinates are called Tortoise coordinates, for which the horizon is located at $z^\star \to -\infty$. $g_{\mu\nu}$ is given by:

$$g_{\mu\nu} = \text{diag}\left(\frac{-f(z)}{z^2}, \frac{f(z)}{z^2}, \frac{1}{z^2}, \frac{1}{z^2}, \frac{1}{z^2}\right) \tag{B.12}$$

This metric and ϕ will again be plugged into the Klein-Gordon equation. This gives:

$$\frac{z^2}{f(z)}\omega^2 b(z) - z^2\vec{k}^2 b(z) + \frac{z^5}{f(z)}\partial_{z^\star}\left(\frac{1}{z^3}\partial_{z^\star} b(z)\right) = 0 \tag{B.13}$$

In order to impose the boundary condition at the horizon we can take the near horizon limit $z \to z_0$, for this limit $f(z) \ll 1$. The first and third term will thus be much larger than the second term. In this limit it is also possible to change $z \to z_0$, which makes it possible to put it in front of the derivative. Neglecting the second term and omitting the overall factor $\frac{z_0^2}{f(z)}$ the equation changes to:

$$\omega^2 b(z) + \partial_{z^\star}^2 b(z) = 0 \tag{B.14}$$

The solution to this equation is:

$$b = a_1 e^{+i\omega z^\star} + a_2 e^{-i\omega z^\star} \tag{B.15}$$

The complete solution is:

$$\phi = e^{i\vec{k}\cdot\vec{x}}\left[c_1 e^{-i\omega t + i\omega z^\star} + c_2 e^{-i\omega t - i\omega z^\star}\right] \tag{B.16}$$

Now the second boundary condition can be imposed. This states that all waves should move towards the black hole centre, $z^\star \to -\infty$. Of the two waves in the above solution only the second wave is moving towards the black hole, so $c_1 = 0$.

The combination of the two boundary conditions will give a unique relation between ω and k. To find the exact dispersion relation the Klein-Gordon equation has to be solved exactly. This will make it possible to combine the two solutions from the boundary conditions and find the dispersion relation. In the example above the two resulting solutions are valid in different regimes (near horizon and AdS-boundary), so they can not be combined to find a dispersion relation.

References

[1] H. Satz. The Quark-Gluon Plasma: A Short Introduction. *Nucl.Phys.*, A862-863:4–12, 2011.

[2] R. Alkofer and J. Greensite. Quark confinement: the hard problem of hadron physics. *J. Phys. G*, 34, 2007.

[3] E. Shuryak. Four lectures on strongly coupled Quark Gluon Plasma. *Nuclear Physics B - Proceedings Supplements*, 195(0):111 – 156, 2009. Proceedings of the 47th Internationale Universittswochen fr Theoretische Physik Fundamental Challenges of QCD 2009.

[4] W. Greiner, D. A. Bromley, S. Schramm, and E. Stein. *Quantum chromodynamics*. Springer Science & Business Media, 2007.

[5] M. E. Peskin and D. V. Schroeder. *An introduction to quantum field theory*. Westview, 1995.

[6] J. Letessier and J. Rafelski. *Hadrons and quark–gluon plasma*, volume 18. Cambridge University Press, 2002.

[7] T.P. Cheng and L.F. Li. *Gauge Theory of Elementary Particle Physics*. Oxford science publications. Clarendon Press, 1984.

[8] F. Wilczek. Asymptotic freedom: From paradox to paradigm. *Proceedings of the National Academy of Sciences of the United States of America*, 102(24):8403–8413, 2005.

[9] D. Banerjee, J. K. Nayak, and R. Venugopalan. Two introductory lectures on high-energy QCD and heavy-ion collisions. In *The Physics of the Quark-Gluon Plasma*, pages 105–137. Springer, 2010.

[10] B. Muller and J. L. Nagle. Results from the relativistic heavy ion collider. *arXiv preprint nucl-th/0602029*, 2006.

[11] J. Blaizot. Theoretical overview: towards understanding the quark-gluon plasma. *arXiv preprint hep-ph/0703150*, 2007.

[12] Robert M Wald. *General relativity*. University of Chicago press, 2010.

[13] L. Susskind and J. Lindesay. *An Introduction to Black Holes, Information and the String Theory Revolution: The Holographic Universe*. World Scientific, 2005.

[14] M. Natsuume. AdS/CFT Duality User Guide. *arXiv preprint arXiv:1409.3575*, 2014.

[15] E. Shuryak. Physics of strongly coupled quark–gluon plasma. *Progress in Particle and Nuclear Physics*, 62(1):48–101, 2009.

[16] J. D. Bekenstein. Black holes and entropy. *Physical Review D*, 7(8):2333, 1973.

[17] D. N. Page. Hawking radiation and black hole thermodynamics. *New Journal of Physics*, 7(1):203, 2005.

[18] S. W. Hawking. Particle creation by black holes. *Communications in mathematical physics*, 43(3):199–220, 1975.

[19] S. W. Hawking. Black holes are white hot. *Annals of the New York Academy of Sciences*, 262(1):289–291, 1975.

[20] O. Aharony, S. S. Gubser, J. Maldacena, H. Ooguri, and Y. Oz. Large N field theories, string theory and gravity. *Physics Reports*, 323(3):183–386, 2000.

[21] M. Fujita and H. Ohki. Geometric entropy and third order phase transition in d=4 N=2 SYM with flavor. *JHEP*, 1008:056, 2010.

[22] P. K. Kundu, I. M. Cohen, and D. R. Dowling. *Fluid Mechanics*. Academic Press, 2012.

[23] T. Springer. Hydrodynamics of strongly coupled non-conformal fluids from gauge/gravity duality. *arXiv preprint arXiv:0908.1587*, 2009.

[24] A. V. Ramallo. Introduction to the AdS/CFT correspondence. In *Lectures on Particle Physics, Astrophysics and Cosmology*, pages 411–474. Springer, 2015.

[25] D. T. Son and A. O. Starinets. Viscosity, black holes, and quantum field theory. *arXiv preprint arXiv:0704.0240*, 2007.

[26] T. Schäfer and D. Teaney. Nearly perfect fluidity: from cold atomic gases to hot quark gluon plasmas. *Reports on Progress in Physics*, 72(12):126001, 2009.

[27] G. Policastro, D. T. Son, and A. O. Starinets. Shear viscosity of strongly coupled N= 4 supersymmetric Yang-Mills plasma. *Physical Review Letters*, 87(8):081601, 2001.

[28] J. Maldacena. The large-N limit of superconformal field theories and supergravity. *International journal of theoretical physics*, 38(4):1113–1133, 1999.

[29] V. E. Hubeny. The AdS/CFT correspondence. *arXiv:1501.00007*, 2015.

[30] T. Faulkner, N. Iqbal, H. Liu, J. McGreevy, and D. Vegh. Holographic non-Fermi-liquid fixed points. *Philosophical Transactions of the Royal Society A: Mathematical, Physical and Engineering Sciences*, 369(1941):1640–1669, 2011.

[31] R. A. Janik. The dynamics of quark-gluon plasma and AdS/CFT. In *From Gravity to Thermal Gauge Theories: The AdS/CFT Correspondence*, pages 147–181. Springer, 2011.

[32] E. Papantonopoulos. *From Gravity to Thermal Gauge Theories: The AdS/CFT Correspondence*. Lecture Notes in Physics. Springer, 2011.

[33] G. Policastro, D. T. Son, and A. O. Starinets. From AdS/CFT correspondence to hydrodynamics. *Journal of High Energy Physics*, 2002(09):043, 2002.

[34] P. K. Kovtun, D. T. Son, and A. O. Starinets. Viscosity in strongly interacting quantum field theories from black hole physics. *Physical review letters*, 94(11):111601, 2005.

[35] S. Aronson and T. Ludlam. Hunting the Quark Gluon Plasma: Results from the First 3 Years at RHIC, rep. no. Technical report, BNL-73847-2005, Brookhaven National Laboratory, Upton, NY (April 2005), available at http://www. bnl. gov/npp/docs/Hunting the QGP. pdf.

[36] E. Shuryak. What RHIC experiments and theory tell us about properties of quark–gluon plasma? *Nuclear Physics A*, 750(1):64–83, 2005.

[37] M. Harrison, T. Ludlam, and S. Ozaki. RHIC project overview. *Nuclear Instruments and Methods in Physics Research Section A: Accelerators, Spectrometers, Detectors and Associated Equipment*, 499(2):235–244, 2003.

[38] D. A. Teaney. Viscous hydrodynamics and the quark gluon plasma. *Quark-Gluon Plasma*, 4:207, 2009.

[39] P. Braun-Munzinger and J. Stachel. The quest for the quark–gluon plasma. *Nature*, 448(7151):302–309, 2007.

[40] P. Huovinen. Hydrodynamics at RHIC and LHC: What have we learned? *International Journal of Modern Physics E*, 22(12):1330029, 2013.

[41] K. H. Ackermann et al. Elliptic flow in Au+Au collisions at $\sqrt{s_{NN}} = 130$ GeV. *Physical Review Letters*, 86:402.

[42] J. Adams et al. Evidence from d+Au Measurements for Final-State Suppression of High-p_T Hadrons in Au+Au Collisions at RHIC. *Physical Review Letters*, 91(7):072304, 2003.

[43] M. Luzum and P. Romatschke. Conformal relativistic viscous hydrodynamics: Applications to RHIC results at $\sqrt{s_{NN}} = 200$ GeV. *Physical Review C*, 78(3):034915, 2008.

[44] H. Song, S. A. Bass, U. Heinz, T. Hirano, and C. Shen. 200 A GeV Au+Au collisions serve a nearly perfect quark-gluon liquid. *Physical review letters*, 106(19):192301, 2011.

[45] H. Song et al. Hydrodynamic modelling for relativistic heavy-ion collisions at RHIC and LHC. *Pramana: Journal of Physics*, 84(5), 2015.

[46] P. Huovinen, P. F. Kolb, U. Heinz, P. V. Ruuskanen, and S. A. Voloshin. Radial and elliptic flow at RHIC: further predictions. *Physics Letters B*, 503(1):58–64, 2001.

[47] E. Shuryak. Heavy Ion Collisions: Achievements and Challenges. *arXiv preprint arXiv:1412.8393*, 2014.